Coordination Chemistry Reviews 549 (2026) 217287

Contents lists available at ScienceDirect

Coordination Chemistry Reviews

journal homepage: www.elsevier.com/locate/ccr

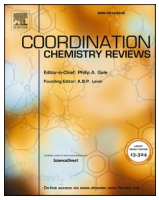

Advances in the design and fabrication of flexible, wearable, and implantable electrochemical neurotransmitter sensors☆

K. Theyagarajan [a,b,*], Laraib Zahra [b], Young-Joon Kim [a,b,*]

[a] Department of Electronic Engineering, Gachon University, Seongnam 13120, Gyeonggi-Do, South Korea
[b] Department of Semiconductor Engineering, Gachon University, Seongnam 13120, Gyeonggi-Do, South Korea

ARTICLE INFO

Keywords:
Neurotransmitter
Electrochemical sensor
Flexible sensor
Wearable sensor
Implantable sensor
Modified electrode
Real-time monitoring

ABSTRACT

Neurotransmitters (NTs) are chemical messengers that play essential roles in the human body, influencing processes such as digestion, mood regulation, memory, learning, heart rate, muscle movement, sleep patterns, blood pressure, and so forth. Maintaining optimal levels of these NTs is essential for normal physiological functioning. Conversely, imbalances in NT levels are frequently associated with various neurological and neurodegenerative disorders, including dementia, Parkinson's, and Alzheimer's disease. Therefore, accurate quantification of NTs in bodily fluids is essential for understanding brain function and the progression of related diseases. Among the various detection technologies available, electrochemical sensors stand out due to their high sensitivity, selectivity, rapid response, low sample volume requirements, and real-time detection capabilities. Furthermore, these sensors can be miniaturized and integrated into portable formats, facilitating the development of wearable, point-of-care (PoC), and implantable electrochemical sensors. These advanced technologies not only enhance patient care but also enable autonomous monitoring, instantaneous data acquisition, and analysis. Thus, we sought to write a concise review focusing on recent advances in materials design and engineering for electrochemical NT sensors. Special emphasis is placed on flexible, wearable, and implantable sensor platforms, as they are particularly promising for real-time applications. To the best of our knowledge, no existing review comprehensively addresses these aspects. Advancing research in this direction may usher in a new era of dynamic NT monitoring, offering improved understanding of the occurrence and development of brain diseases and their treatment outcomes.

Abbreviations: AA, Ascorbic acid; AAD, 2-Aminoadenosine; AAHG, Amyloid albumin hydrogels; ACh, Acetylcholine; ADHD, Attention-deficit hyperactivity disorder; ADO, Adenosine; AgNPs, Silver nanoparticles; AgNWs, Silver nanowires; AMP, Amperometry; ASD, Autism spectrum disorder; AuNPs, Gold nanoparticles; AuNWs, Gold nanowires; BSA, Bovine serum albumin; CB, Carbon black; CC, Carbon cloth; C-C, Conductive carbon; CFE, Carbon fiber electrode; CNC, Cellulose nanocrystal; CNR, Carbon nanorods; CNS, Central nervous system; CNSs, Carbon nanostructures; CNT, Carbon nanotube; CS, Chitosan; CSF, Cerebrospinal fluid; CV, Cyclic voltammetry; CVD, Chemical vapor deposition; CY, Carbon yarn; DA, Dopamine; DMSO, Dimethyl sulfoxide; DPV, Differential pulse voltammetry; E:I, Excitatory and inhibitory; EDRF, Endothelium-derived relaxing factor; ELSD, Early-life sleep disruption; EP, Epinephrine; ERGO, Electrochemically reduced graphene oxide; FSCV, Fast-scan cyclic voltammetry; GABA, 4-Aminobutyric acid; GluOx, Glutamate oxidase; GNCs, Gold nanoclusters; GO, Graphene oxide; GP, Graphite powder; GR, Graphene; HUVECs, Human umbilical vein endothelial cells; IL, Ionic liquid; IMS, Implantable sensor; ISF, Interstitial fluid; ITO, Indium tin oxide; L-Glu, L-Glutamate; LIG, Laser-induced graphene; LOD, Limit of detection; LSG, Laser-scribed graphene; MB, Methylene blue; MEAs, Microelectrode arrays; MIP, Molecularly imprinted polymer; MOF, Metal-organic framework; m-SWCNT, Metallic single-walled carbon nanotubes; MWCNTs, Multiwalled carbon nanotubes; NE, Norepinephrine; NF, Nafion; NHNFs, Nickel hydroxide nanoflakes; NMDA, *N*-methyl-D-aspartate; NO, Nitric oxide; NP, Nail polish; NPs, Nanoparticles; NPt, Nano platinum; NT, Neurotransmitter; NTLO, Sodium titanium layered oxide; OHP, Overhead projector; PANI, Polyaniline; PB, Prussian blue; PBA, Phenylboronic acid; PBS, Phosphate buffer saline; PDMS, Polydimethylsiloxane; PE-CVD, Plasma-enhanced chemical vapor deposition; PEDOT, Poly(3,4-ethylenedioxythiophene); PEI, Polyethyleneimine; PEN, Poly(ethylene naphthalene); PET, Polyethylene terephthalate; PLA, Poly(lactic acid); PMMA, Poly(methyl methacrylate); PoPD, Poly-*o*-phenylenediamine; PmPD, Poly-*m*-phenylenediamine; PPY, Polypyrrole; PSS, Polystyrene; pTA, Poly(tannic acid); PTMC, Poly(trimethylene carbonate); PtNPs, Platinum nanoparticles; PVA, Polyvinyl alcohol; PVC, Polyvinyl chloride; RGO, Reduced graphene oxide; ROS, Reactive oxygen species; SAC, Single-atom catalyst; SAM, Self-assembled monolayer; S-CNTFs, Spindle-shaped carbon nanotube fibers; SPCE, Screen-printed carbon electrode; SPE, Screen-printed electrode; SPGE, Screen-printed graphene electrodes; SS, Stainless steel; SSB, Sulfonated poly(styrene-butadiene) flexible fiber membrane; STN, Serotonin; SWV, Square wave voltammetry; UA, Uric acid; ULTS, Ultra-large tunable stiffness; VG, Vertical graphene; WGP, WS_2/graphene heterostructure on polyimide; WS, Wearable sensor.

☆ This article is part of a Special issue entitled: 'Molecules and Devices: CCMD' published in Coordination Chemistry Reviews.

* Corresponding authors at: Department of Electronic Engineering, Gachon University, Seongnam 13120, Gyeonggi-Do, South Korea.
E-mail addresses: thektr@gachon.ac.kr (K. Theyagarajan), youngkim@gachon.ac.kr (Y.-J. Kim).

https://doi.org/10.1016/j.ccr.2025.217287
Received 3 October 2025; Accepted 14 October 2025
Available online 24 October 2025

1. Introduction

Neurotransmitters (NTs) are small molecules that function as chemical messengers by transmitting, enhancing, or inhibiting signals between neurons, or between neurons and other target cells [1,2]. They are integral to the central nervous system (CNS) and play a crucial role in regulating a wide range of physiological functions, including heart rate, respiration, digestion, sleep patterns, mood, memory, learning, muscle movement, appetite, and more [3,4]. The first neurotransmitter, acetylcholine, was discovered by Nobel Laureates Henry Dale and Otto Loewi [5]. Since then, over 100 NTs have been identified, with ongoing discoveries expanding our understanding. A detailed classification of NTs based on their molecular structures is schematically illustrated in Fig. 1. Each NT performs specific roles: excitatory NTs stimulate target cells, inhibitory NTs suppress action, and modulatory NTs influence multiple neurons simultaneously. Additionally, NT functions are receptor-specific, with biological effects depending on the receptor type to which the NT binds [6–8]. Maintaining optimal NT concentrations is essential for both physiological and mental health. Imbalances are often linked to neurological and psychiatric disorders such as dementia, depression, schizophrenia, Parkinson's disease, Alzheimer's disease, and other neurodegenerative conditions [9–11]. Therefore, accurate detection of NTs is essential for the early diagnosis and effective intervention of these often-incurable diseases, potentially improving treatment outcomes through timely management [12,13].

Numerous detection techniques have been used for NT detection, including fluorimetry, radioimmunoassay, capillary electrophoresis, high-performance liquid chromatography, mass spectrometry, magnetic resonance imaging, electrochemical (bio)sensing, chemiluminescence, and enzyme-linked immunosorbent assay. However, most conventional methods are expensive, time-consuming, labor-intensive, and often require complex sample pretreatment [14–16]. Among these, electrochemical techniques stand out due to their rapid response, high sensitivity and selectivity, cost-effectiveness, and ease of operation [17–20]. Electrochemical sensors can also be miniaturized, making them well-suited for integration into wearable and portable devices for continuous, real-time, and on-site monitoring [21,22]. Furthermore, they can be combined into Internet of Things (IoT) systems, enabling remote sensing, autonomous monitoring, and real-time alerts for abnormal conditions to be sent to users or healthcare providers [23]. Some of the commonly used electrochemical techniques for NT detection include amperometry (AMP), differential pulse voltammetry (DPV), square wave voltammetry (SWV), and fast-scan cyclic voltammetry (FSCV) [24]. In general, electrochemical sensing utilizes a three-electrode system consisting of a working electrode (WE), a reference electrode (RE), and a counter electrode (CE), with the reaction of interest occurring at the WE. Conventional metallic or carbon electrodes often suffer from limited selectivity and require high operational potential [25,26]. To overcome these limitations, surface modification strategies have been employed, where the WE is functionalized with various functional materials and molecules to improve selectivity, enhance sensitivity, and reduce operating voltages [27]. A wide range of advanced materials and functional molecules have been explored for electrode surface modification, including carbon nanomaterials, metal nanoparticles, organic frameworks, quantum dots, ionic liquids, redox molecules, and more [28–32]. The physicochemical properties of these materials play a critical role in determining the sensor performance, stability, and applicability [33]. Another important research direction involves optimizing electrode shapes and configurations. The geometry of electrodes has a significant influence on sensor functionality and feasibility. Rigid electrodes are unsuitable for flexible and wearable sensors due to their inability to bend or conform to dynamic surfaces [34,35]. In response to this emerging demand, researchers worldwide are developing custom-designed, flexible substrate-based electrodes for wearable and implantable sensor applications [36,37].

Despite numerous studies on flexible electrochemical NT sensors, only a few have focused explicitly on wearable and implantable formats. This gap in the literature motivated us to investigate the opportunities and challenges in advancing flexible sensors toward wearable and implantable platforms. Based on our comprehensive literature survey and understanding, no prior review has specifically addressed the development of flexible, wearable, and implantable electrochemical sensors for NT detection. This review aims to fill that gap by highlighting the significance of these technologies. We examine key fabrication components, their influence on sensor performance, current advantages and limitations, and propose strategies for future research. This review is organized analyte-wise to help researchers easily identify progress made in detecting specific NTs. Overall, we hope this work will serve as a foundation for the development of high-throughput wearable and implantable sensors for real-time NT monitoring, ultimately

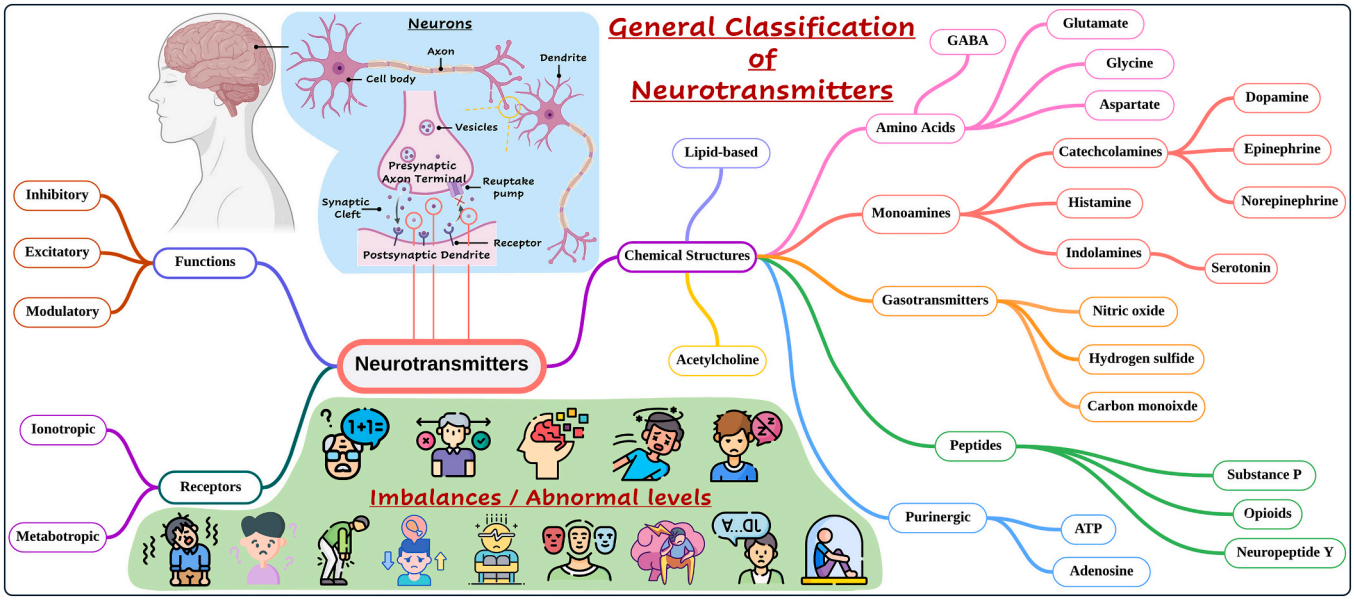

Fig. 1. General classification of neurotransmitters based on their chemical structures and their significance in human physiology. Part of this image has been created using the icons from biorender.com and flaticon.com.

contributing to a better understanding and more effective treatment of various brain-related disorders.

2. Electrochemical-based flexible, wearable, and implantable sensors for neurotransmitter monitoring

2.1. Amino acid NTs

Amino acid NTs are among the most predominant and functionally significant NTs, playing key roles in fundamental brain processes such as cognition, consciousness, arousal, and sleep. They are also critically involved in the pathogenesis of neurological disorders such as dementia, epilepsy, and stroke, which disrupt these functions. Structurally, they are simple molecules characterized by an ammonium cation and a carboxylate anion at opposite ends. Some of the well-known amino acid NTs include glycine, L-glutamate, and GABA.

2.1.1. GABA

4-Aminobutyric acid, also known as ɣ-aminobutyric acid (GABA), is a primary inhibitory NT essential for normal brain function. An imbalance in GABA levels has been associated with depression and other affective disorders, emphasizing the importance of accurate detection in the human body [38]. Moreover, recent studies suggest that brain changes associated with autism spectrum disorder (ASD) involve increased glutamatergic excitation and reduced GABAergic inhibition, further highlighting the need for real-time monitoring of GABA. In a recent study, Li and coworkers developed a molecularly imprinted polymer (MIP)-based flexible electrochemical sensor for the selective detection of GABA [39]. The sensor was fabricated by modifying an indium tin oxide (ITO)-polyethylene terephthalate (PET) electrode with magnetically functionalized reduced graphene oxide (RGO). To enhance selectivity, a molecular imprinting approach was employed using 2,4-dinitrofluorobenzene-GABA as the template molecule and pyrrole as both the functional monomer and cross-linking agent. The MIP was formed via electropolymerization, followed by template removal through stirring elution, resulting in specific recognition sites for GABA. Experimental validation was carried out by measuring GABA levels in the serum of depressed mouse models induced by chronic unpredictable mild stress. The results revealed that GABA levels were significantly lower in the depressed groups compared to the control groups, confirming the sensor's potential for use in depression diagnosis. Similarly, Chu and the group designed a flexible micro-biosensor for the simultaneous real-time detection of GABA and L-glutamate [40]. As L-glutamate and GABA are excitatory and inhibitory (E:I) NTs, their imbalance is strongly associated with various neurological disorders, including ASD, and is crucial for understanding the neural mechanisms underlying these conditions. The sensor was fabricated on a polyimide (PI) substrate, which allowed for easy handling and minimized brain damage during implantation. Pt-black nanostructures were incorporated to enhance the active surface area and sensitivity, while also providing a conductive surface for the covalent immobilization of glutamate oxidase (GluOx) and GABase. Here, Pt-black improved the surface roughness at the microscale level and expanded the electroactive surface area, which boosted electron transfer and sensitivity. Although the sensor employed biocatalysts to enhance the specificity, its linear range and detection limit were severely compromised compared to those of MIP-based sensors. Further, to improve the anti-biofouling property of the sensor, a size-exclusion layer was formed using poly-*m*-phenylenediamine (PmPD). The sensor's performance was initially evaluated through in vitro and ex vivo tests using glutamatergic neuronal cells, followed by in vivo validation in anesthetized rat brains. These results demonstrate high selectivity, sensitivity, and the capability of real-time monitoring. Furthermore, the sensor was proposed for use in early-life sleep disruption (ELSD) models, which are associated with E:I imbalance in ASD. This advancement represents a powerful tool for real-time neurochemical sensing, offering new opportunities to explore brain function and the pathophysiology of neurological disorders.

2.1.2. Glycine

Glycine is also an inhibitory neurotransmitter primarily found in the brainstem, spinal cord and retina. It plays a critical role in processing motor and sensory information, facilitating functions such as audition, vision and movement. In addition to its inhibitory function, glycine also acts as a co-agonist at *N*-methyl-D-aspartate (NMDA) subtype receptors. Due to its vital physiological role, the sensitive detection of glycine is crucial [41]. To date, no wearable or flexible sensor has been reported for the selective detection of glycine alone. However, Ling and colleagues developed a flexible and implantable sensor capable of detecting glycine alongside other nutrients, including glucose, ascorbic acid and L-tryptophan [42]. The home-made flexible sensor was printed using a high-throughput screen printing technique on a PET substrate, incorporating multiple layers of carbon, polymeric insulators, and silver inks, as shown in Fig. 2B. To enhance the sensing performance, the sensors were modified by drop-casting cobalt and copper metal-organic framework (MOF) nanoparticles (NPs), followed by a layer of Nafion (NF) solution (Fig. 2C). The sensors featured sharp tips to facilitate implantation into tissues and organs, while their thin and flexible structure allowed them to access interstitial fluids (ISF) and conform to various organs with complex geometries. The incorporation of MOF significantly improved the stability, biocompatibility, and operational longevity of the proposed sensor. This platform offers promising potential as either a single- or multichannel device for real-time monitoring across various organs.

2.1.3. L-glutamate

L-Glutamate (L-Glu), the anionic form of glutamic acid, is the primary and most abundant excitatory neurotransmitter in the vertebrate nervous system. It is one of the most extensively studied NTs, and it plays a crucial role in numerous physiological processes, including memory, neural development, learning, synaptic plasticity, emotional regulation, behavior, and signal transmission [43]. Additionally, it is essential for bioenergetic and biosynthetic pathways, as well as cellular metabolism. L-Glu is also involved in the transmission of signals related to pain and vision. Abnormal levels of L-Glu have been associated with various health conditions, such as attention deficit hyperactivity disorder (ADHD), seizures, and excitotoxicity. Moreover, dysregulation of L-Glu is implicated in the pathophysiology of severe neurological and psychiatric disorders, including Alzheimer's disease, stroke, autism, multiple sclerosis, schizophrenia, and depression. Given its critical functions, maintaining optimal L-Glu levels is essential for overall brain function and health [44].

Weltin and the team developed a flexible microsensor using a Pt-coated polymer substrate for the in vivo electrochemical monitoring of L-Glu and lactate for the first time [45]. This sensor featured a polymer strip with two working electrodes positioned at its tip, designed for direct insertion into tissue without the need for guiding instruments. The core structure consisted of a 50 μm thick PI film, coated on both sides with a 5 μm thick epoxy insulation layer and a 38 μm thick dry film resist layer, resulting in an overall thickness of approximately 100 μm and a width of 500 μm (Fig. 3A&B). Thereafter, a thin layer of metallized Pt was coated onto the PI substrate. The enzyme was then immobilized on the electrode within a membrane, while hydrogels were applied as a diffusion barrier. This metallized Pt-based sensor offers a comparatively smaller active surface area than the Pt-black–modified sensor [40], which restricts the number of catalytic sites available for electron transfer. As a result, simple Pt metallization falls short of delivering the high sensitivity and rapid response achieved with Pt-black. This underscores the pivotal role of electrode surface architecture in governing the structure–activity relationship and overall sensor performance. Furthermore, a perm-selective membrane composed of 1,3-diaminobenzene was applied to the WEs during the wafer-level manufacturing process to improve the selectivity. The sensors were fabricated in

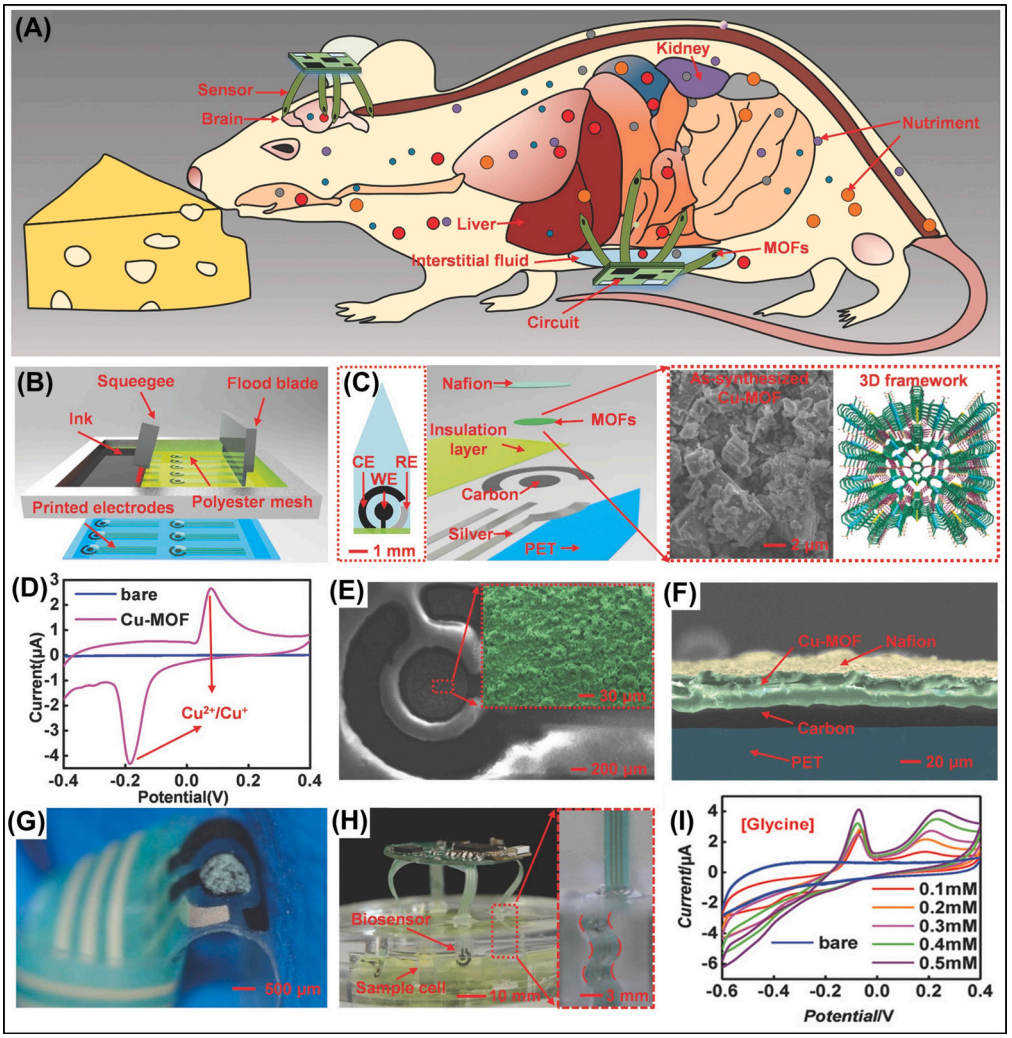

Fig. 2. (A) Conceptual illustration of the flexible MOF sensor application. (B) Schematic of the screen-printing process. (C) Exploded view showing various layers of the MOF sensor, along with SEM micrograph and 3D framework of Cu-MOF. (D) CVs of bare and Cu-MOF sensors in PBS. (E) SEM image of MOF-modified sensor. (F) Sectional view of the sensor. (G) Photograph of the flexible MOF sensor in a bent state. (H) Photograph of the PDMS microfluidic device integrated with flexible MOF sensors. (I) CVs of bare and Cu-MOF sensors for different glycine concentrations. Reproduced with permission from [42].

different lengths for specific applications (Fig. 3C&D): shorter ones provided rigidity for brain insertion, while longer variants offered flexibility for subcutaneous and intramuscular implantation. Moreover, the sensor achieved a rapid response time, reaching 95% of the signal within 5 s after the addition of 10 mM L-Glu. In a subsequent development, Nguyen and the team fabricated an L-Glu biosensor by immobilizing GluOx on nanocomposite electrodes composed of platinum nanoparticles (PtNPs), multiwalled carbon nanotubes (MWCNTs), and PEDOT:PSS, all printed on a flexible substrate [46]. The fabrication process involved mixing functionalized MWCNTs and PtNPs in DMSO via sonication, followed by the addition of PEDOT:PSS ink and Ecoflex to achieve a suitable viscosity for printing. The composite ink was dispensed using a 3-axis microfluid dispensing robot equipped with glass capillary pipettes to define the WE, CE, and conductive traces. Ag/AgCl ink was used for the RE and contact pads, while polydimethylsiloxane (PDMS) insulation was applied, leaving only the electrodes and contact pads exposed. After which, the WE were coated with an enzyme matrix containing GluOx, bovine serum albumin (BSA), and glutaraldehyde, and finally covered with an NF layer to enhance its selectivity. The sensor was successfully implanted in the spinal cord of rats, where it effectively quantified L-Glu release following spinal cord injury. Overall, the implantable biosensors demonstrated excellent sensitivity, selectivity, flexibility, repeatability, and stability, making them promising tools for in vivo neurochemical monitoring.

In another study, Wen and colleagues developed a highly flexible and versatile neural probe capable of deep brain implantation without the need for external shuttle carriers or coatings for sensing and drug delivery [47]. This flexible and stretchable probe incorporates ultra-large tunable stiffness (ULTS) and features a compact, free-standing, multilayer structure composed of 30 μm-thick PDMS, integrating Pt electrodes, microfluidic channels, and electrical interconnects. PDMS was selected for its low Young's modulus, high stretchability, and biocompatibility. During fabrication, Pt electrodes, soldering pads, and SiO_2 insulating layers were patterned on a silicon substrate, which served as a sacrificial layer. A PDMS thin film was deposited and patterned via a lift-off process, forming connections between the electrodes at the probe tip and the base while simultaneously passivating the electrical interconnects and microfluidic channels. A second PDMS layer containing microfluidic channels was then bonded to the first layer using O_2 plasma, followed by a third PDMS layer incorporating stiffening channels (Fig. 3E). Liquid gallium (Ga) was injected into the interconnects and stiffening channels and subsequently frozen to retain structural rigidity after XeF_2 release. The entire probe was then released from the silicon substrate through XeF_2 undercutting, resulting in a 2 cm single-shank ULTS probe. The solid-to-liquid phase transition of Ga at body temperature enabled a temperature-dependent control of stiffness across

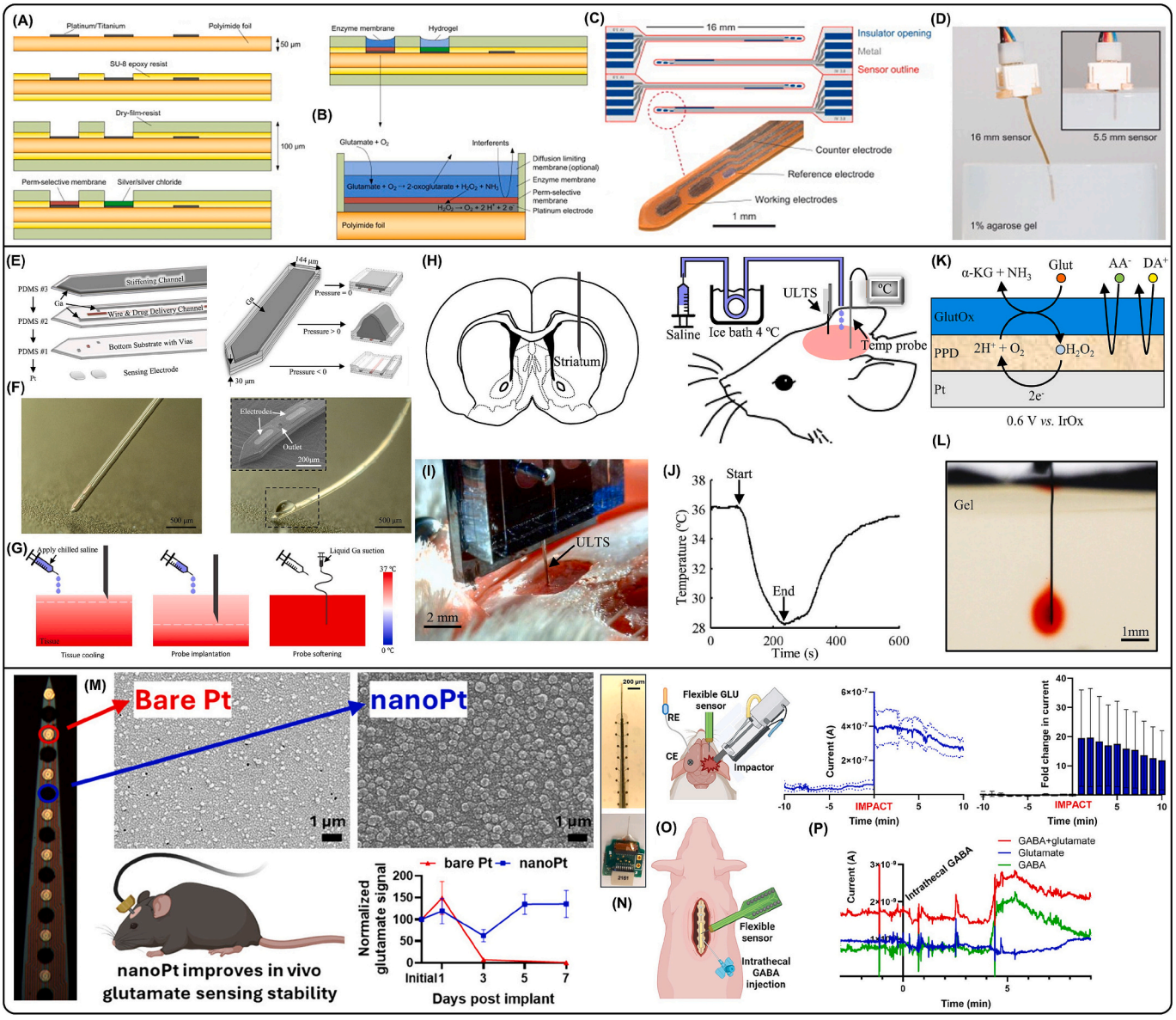

Fig. 3. (A & B) Graphical cross-sectional illustration of the fabrication steps for the flexible sensor (C) Photograph of the flexible sensor and (D) the sensor immersed in agarose gel. Reproduced with permission from [45]. (E) Graphical representation of various layers of the ULTS probe. (F) Photographs of the ULTS probe in its stiff and soft states with integrated drug delivery. Inset: SEM image of the ULTS probe showing the electrodes and outlet opening. Schematics of the implantation procedure (G) in a brain phantom (0.6% agarose gel) and (H) in a rat brain. (I) Photograph of the ULTS probe implanted in the rat brain. (J) Temperature profile illustrating cooling and temperature recovery in a rat brain following the application of a chilled saline solution. (K) Schematic illustration of the multilayer structure of the L-Glu sensor and its electrocatalytic sensing mechanism. (L) Photograph of liquid delivery using the ULTS probe. Reproduced with permission from [47]. (M) Photograph and SEM images of the NPt neural probe. (N) Photograph of the MEA attached to the home-made PCB. (O) Graphical representation of L-Glu measurement in animal models and (P) the corresponding electrochemical responses. Reproduced with permission from [43].

five orders of magnitude. In its stiff state, the probe was successfully inserted 2 cm deep into agarose gel (0.6%) "brain phantoms". Once the Ga melted, the ULTS probes became ultra-soft, highly flexible, and stretchable in all directions (Fig. 3G). The Pt microelectrodes were fabricated on thin silicon dioxide islands on a separate silicon wafer and subsequently transferred to the ULTS probe to ensure stable electrical connections. Then, a PmPD layer was incorporated to achieve high selectivity with a mechanically adaptable design, allowing for deep-brain implantation with minimal tissue damage. Although these flat Pt surfaces exhibit only moderate catalytic efficiency compared to Pt-black [40] or nano-Pt [43], these findings demonstrate that nano- or micro-structuring of Pt can significantly enhance sensitivity. For biosensing functionality, the sensors were further modified with GluOx, BSA, and glutaraldehyde. During implantation in animal models, the brain tissue was temporarily cooled by applying chilled saline to the skull surface, a common method for local, reversible neuronal inhibition and neuroprotection (Fig. 3H&I). After implantation, Ga melted as the tissue temperature returned to normal, allowing the probe to become soft and compliant with brain tissue (Fig. 3J).

Recently, Poolakkandy and the team developed a flexible, non-enzymatic electrochemical sensor for effective glutamic acid detection using nickel hydroxide nanoflakes (NHNFs) incorporated with MWCNTs [44]. The initial performance evaluation was conducted using NHNFs-MWCNT/GCE, which showed excellent electrocatalytic activity toward glutamic acid detection, even in the presence of various interfering substances. Thereafter, a flexible sensor was developed by coating this electrocatalyst over a pyrolytic graphite sheet affixed to a polyester film and utilized to monitor glutamic acid released by human neural cells and

monosodium glutamate in food samples. The sensor successfully quantified the glutamic acid released by SH-SY5Y cells under both normal conditions and oxygen-glucose deprivation stress, demonstrating its potential for clinical and biomedical applications. In a recent study, Robbins and the team developed an enhanced enzymatic L-Glu sensor using Pt electrodes with nanometer-scale roughness created by nano platinum (NPt) electrodeposition [43]. The sensor was fabricated by electrodepositing NPt onto a Pt disk electrode, followed by coating with PmPD, BSA, glutaraldehyde, and GluOx. The resulting sensor demonstrated excellent electrocatalytic activity, stability, and sensitivity for in vitro L-Glu analysis. Here, incorporation of NPt significantly increased the surface roughness, enhancing the number of available anchoring sites for enzyme immobilization. This modification resulted in a 67.4% increase in sensitivity and prolonged stability for up to 3 weeks, compared to a smooth Pt sensor. The sensor was further validated for in vivo analysis by evaluating L-Glu concentrations in a rat model of traumatic brain injury in the striatum. The implanted NPt sensor produced detectable signals during brain injury and maintained a strong response for 7 days, whereas the smooth Pt sensor lost all signals within 3 days of implantation (Fig. 3M). Additionally, the versatility of the NPt sensor was demonstrated by its successful application in measuring GABA levels in the porcine thoracic spinal cord. Overall, the NPt sensor represents a robust and highly sensitive platform for in vivo enzymatic detection of various NTs. Similarly, a comparable response was observed while involving Pt black in the sensor interface [40]. In both studies, electrochemical sensitivity, selectivity, and kinetics are linked to surface morphology, active site density, and electrode-analyte interactions. This clearly shows a structure-activity relationship, where modifications at micro- or nanoscale levels directly enhance sensing performance. Table 1 summarizes the analytical performances of various amino acid-based NT sensors. As per the Scopus literature survey, there are currently no reported flexible, wearable, or implantable electrochemical sensors for other amino acid NTs. This gap presents a significant opportunity for researchers to explore and develop novel sensors in this promising area of study.

2.2. Monoamine NTs

Monoamines are essential classes of NTs that play diverse roles in the nervous system and regulate numerous brain functions, including consciousness, cognition, emotion, arousal, sleep mechanisms, hormone secretion, and gastrointestinal control. Abnormalities in monoamine levels are closely associated with various psychiatric and neurological disorders such as depression, anxiety, Parkinson's disease, and more. Some of the well-known monoamine NTs include dopamine, serotonin, epinephrine, and norepinephrine.

2.2.1. Dopamine

Dopamine (DA) is a catecholamine neurotransmitter and a widely distributed neurohormone in the mammalian CNS. It plays a vital role in neurotransmission and is involved in regulating cardiovascular and renal functions, as well as various other physiological processes. Abnormal DA levels are associated with several neurological disorders, including ADHD, Parkinson's disease, schizophrenia, and drug addiction. Conversely, reduced DA levels are linked to fatigue, depression, and decreased motivation. Therefore, the sensitive and selective detection of DA is highly significant for understanding the underlying mechanisms of neurological conditions and evaluating treatment outcomes [48,49].

Ohno and coworkers developed a flexible DA sensor using SWCNT microelectrodes [50]. Here, the SWCNTs were electrochemically functionalized in sulfuric acid, enhancing the electron transfer rate without compromising the potential window. This modification significantly improved the detection limit to 100 nM, compared to 1 μM for the pristine electrode. The introduction of oxygen-functional groups on the SWCNT surface played an essential role in boosting the electron transfer kinetics and DA sensing capabilities. In a follow-up study, the same group developed another SWCNT-based flexible DA sensor using the dry transfer process based on floating catalyst chemical vapor deposition (FC-CVD) [51]. Here, the clean SWCNT films were prepared, deposited onto a plastic substrate, and covered with an oxide layer to prevent contamination. The resulting microelectrodes demonstrated near-ideal electrochemical behavior, with an average quartile potential difference of 60.4 mV across 28 sensors. Additionally, the microelectrodes demonstrated superior resistance to surface fouling during DA oxidation, showing only 1.8% degradation in oxidation current after 10 cycles compared to 8.3% for the carbon fiber electrode (CFE) and 13.9% for gold electrodes. Compared to the introduction of the oxygen functional group [50], the oxide layer-covered SWCNT sensor provided excellent uniformity, high sensitivity, and reproducibility, and achieved a better LOD.

In another work, a spindle-shaped CNT fibers (S-CNTFs) were synthesized using an electrochemical expansion approach and employed for the simultaneous detection of DA, UA, and AA [52]. The synthesis was

Table 1
Analytical performances of various amino acid-based NT sensors.

Sensors	Substrates	Types	Analyte	Linear range (μM)	LOD (nM)	Sensitivity (nA μM^{-1} mm^{-2})	Techniques	Real samples	Ref.
MIP/MRGO/ITO	PET	Flexible / Implantable	GABA	2.5×10^{-4}–100	12.5×10^{-2}	–	DPV	Depressed mice serum	[39]
GABase/PmPD/Pt-black	Polyimide	Flexible / Implantable	GABA	10–100	40	1.34	AMP	Neuronal cells and rat brain	[40]
GluOx/PmPD/Pt-black			L-Glu	5–100	120	1.74	AMP		
NF/Cu-MOF	PET	Flexible / Implantable	Glycine	100–500	710	–	CV	–	[42]
GluOx/PmPD/NanoPt	Polyimide	Flexible / Implantable	L-Glu	10–1000	–	1.59×10^{-2}*	AMP	Rat brain	[43]
GABase/PmPD/ NanoPt			GABA		–	–		Porcine thoracic spinal cord	
NHNFs/MWCNT/ pyrolytic graphite	Polyester	Flexible	L-Glu	1–1000	72	309.80*	CV	SH-SY5Y neural cells	[44]
GluOx/Pt	Polyimide	Flexible	L-Glu	Up to 150	220	2.16	AMP	Rat brain	[45]
NF/GluOx/PtNPs/ MWCNTs/ PEDOT: PSS	PDMS	Flexible / Implantable	L-Glu	1–800	500	2.60	AMP	Rat spinal cord	[46]
GluOx/PtNPs/ MWCNTs/ PEDOT: PSS				10–600	200	12.80		–	
GluOx/PmPD/Pt	PDMS	Flexible / Implantable	L-Glu	Up to 160	390	8.2×10^{-3}*	FIA	Rat brain	[47]

GluOx – Glutamate oxidase; ITO - Indium tin oxide; MIP - Molecularly imprinted polymer; MRGO - Magnetically functionalized reduced graphene oxide; NHNFs - Nickel hydroxide nanoflakes; PET - Polyethylene terephthalate; PmPD - Poly-*m*-phenylenediamine. *nA μM^{-1}

performed in a one-step process at a liquid-air interface using a two-electrode system, as shown in Fig. 4A. This method produced macroscopic S-CNTFs with a 5000-fold volume expansion, resulting in excellent conductivity, mechanical stability, and a high specific surface area. The S-CNTFs sensor exhibited excellent performance in both sensing and energy storage applications. Finally, the S-CNTFs were woven into a fabric to develop a wearable sensor interface, which, on sweat analysis, showed comparable performance to that of HPLC (Fig. 4C). Moreover, the S-CNTFs based DA sensor exhibited a broader linear range and higher sensitivity compared to f-SWCNT and oxide/SWCNT sensors discussed earlier. Ghosh and team developed a novel flexible sensor using laser-induced graphene (LIG) for the detection of DA and interleukin (IL-6) [53]. The sensor was fabricated through a one-step laser processing technique on Kapton film, followed by surface modification using graphene (GR), PEDOT:PSS, and PANI inks. Among the tested configurations, the LIG/G-PANI exhibited a low detection limit, along with superior sensitivity and selectivity compared to the LIG/G-PEDOT:PSS, SPE/G-PEDOT:PSS, and SPE/G-PANI-based sensors for DA sensing. The superior performance of the LIG/G-PANI sensor could be attributed to the increase in its effective surface area, which was 382% and 488% higher than that of bare SPE and LIG, respectively. In another study, a bacteria-templated synthesis approach was employed to produce porous nitrogen-doped carbon nanorods (CNRs) decorated with AuNPs for DA detection [54]. The incorporation of AuNPs and N-doping enhanced the catalytic active sites and effective surface area, thereby providing a broader linear range and lower detection limits compared to the previously discussed sensors.

A wearable microneedle sensor was developed for the continuous monitoring of DA using a nanocomposite composed of GO, Fe_3O_4 NPs, and chitosan (CS) [55]. The microneedles were fabricated from poly (methyl methacrylate) (PMMA), coated with the nanocomposite, and subsequently covered with an NF layer to enhance selectivity. The sensor showed excellent electrocatalytic activity with a low LOD for DA, delivering stable, reliable, and sensitive performance over time. Additionally, the sensor was successfully evaluated in a skin-mimicking phantom model and artificial ISF, demonstrating acceptable and consistent results. Similarly, another microneedle-based flexible DA sensor was developed using ZnO-coated, Au-sputtered PDMS microelectrode arrays [56], which exhibited comparable analytical performance to the previously reported iron oxide-modified microneedle sensor.

Qing and coworkers developed a high-performance wearable sensor using polypyrrole (PPY), GR, NF, and RGO deposited onto cotton@PET for the ultrasensitive detection of DA, lactate, and glucose [57]. The cotton@PET substrate was plasma-treated to enhance its hydrophilicity, then it was coated with GO and PPY via plasma-enhanced CVD (PE-CVD), followed by the application of NF coating to yield the desired fiber sensor (Fig. 4D). This obtained fiber was subsequently knitted into a fabric and employed for detecting the target analytes (Fig. 4E). The sensor incorporated with GR exhibited better sensitivity, albeit at the cost of a reduced linear range compared with the sensor without GR. Additionally, the sensor was tested for real-time sensing in both artificial and real sweat, demonstrating reliable and effective performance. Another conductive fabric was developed using S-GO, polyvinylidene fluoride, and *N*-methyl-2-pyrrolidone and utilized for the detection of DA, AA, NADH, and UA [58]. Similarly, a fiber-based electrode for DA sensing was developed using RGO electrodeposited onto stainless steel (SS) filaments via a direct electrochemical reduction process [59]. This method eliminated the need for additional surface modifications such as NF coating or electrode oxidation. The strong electrostatic interactions and π–π stacking between RGO and DA enabled high selectivity, even in the presence of common interfering agents. However, although the sensor exhibited a comparable linear range to the previously reported PPY–GR-based sensor, its detection limit was significantly compromised. Furthermore, the sensor showed excellent stability, maintaining its performance after multiple cycles and up to 2 months of storage. For a practical demonstration, the RGO-SS electrodes were successfully integrated into a 3D braided structure and employed as a flexible sensor for DA sensing.

Wang and coworkers developed a microfluidic-based wearable sensor for the detection of DA and UA using a CuNi-MOF decorated RGO [60]. A PI film was used as a flexible substrate, which was then coated with MOF and RGO nanostructures (Fig. 5A). To improve sweat collection, the sensor was integrated with a PDMS-based porous microfluidic device (Fig. 5B), and the components of the wearable sensor are illustrated in Fig. 5C. The incorporation of Cu and Ni in the MOF structure significantly boosted the catalytic activity, while carboxylic acid groups on GO facilitated selective detection. The sensor displayed excellent selectivity with minimal interference, as well as strong repeatability and stability. In another study, Song and coworkers developed a wearable DA sensor with enhanced antifouling and antimicrobial capabilities using MXene and CeO_2 NRs doped amyloid

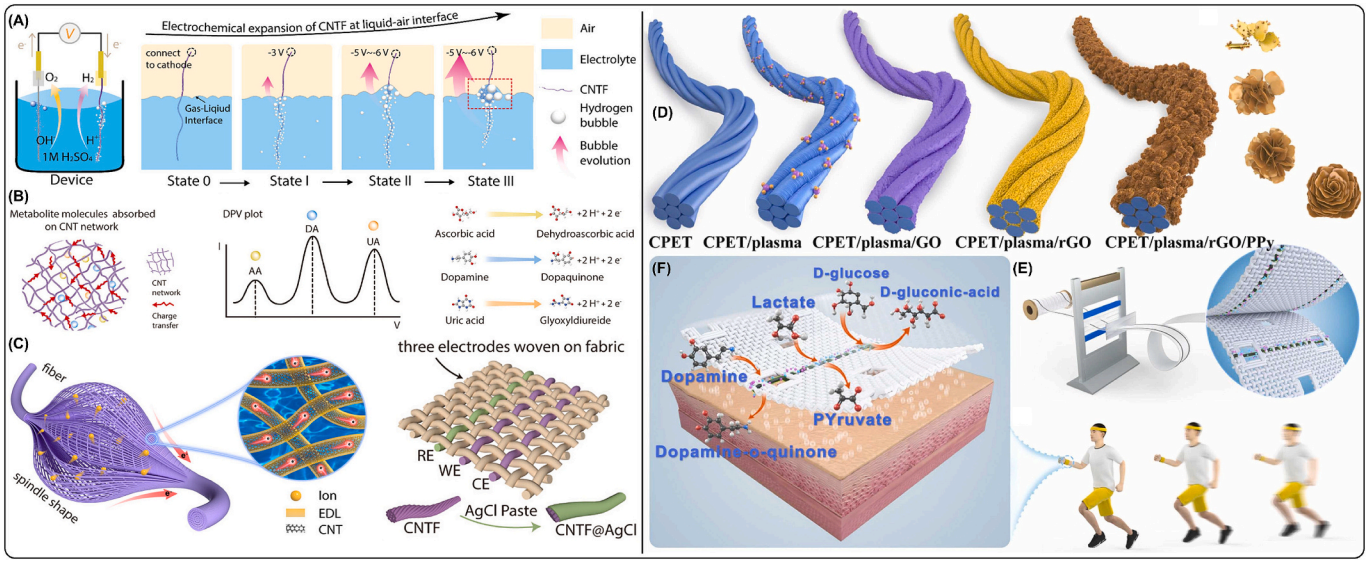

Fig. 4. (A) Graphical illustration of the fabrication of S-CNTFs at the liquid-air interface. (B) Electrochemical performance of the S-CNTFs sensor and its sensing mechanism. (C) Graphical visualization of S-CNTFs and their integration into fabrics. Reproduced with permission from [52]. (D) Scheme of fabric sensor fabrication. (E) Sensor assembly process and (F) corresponding sensing mechanisms. Reproduced with permission from [57].

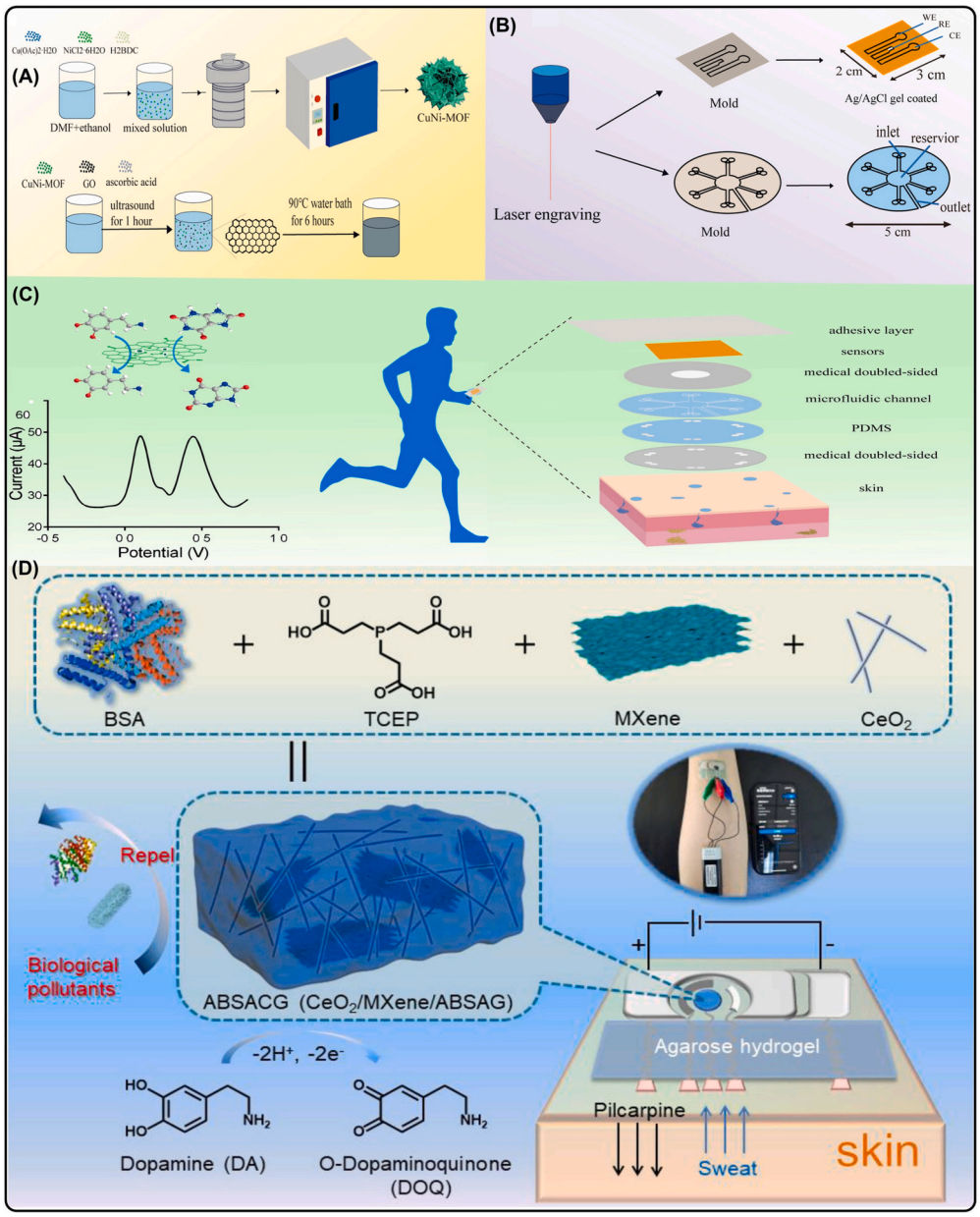

Fig. 5. (A) Scheme for the synthesis of CuNiMOF@RGO. (B) Graphical illustration of the fabrication process for the sensor and microfluidic channel. (C) Exploded view showing the various components of the wearable sensor and its electrocatalytic activity. Reproduced with permission from [60]. (D) Schematic of the hydrogel sensor fabrication and its working mechanism. Inset: Photograph of the wearable sensor. Reproduced with permission from [61].

albumin hydrogels (AAHG) [61]. A schematic of the sensor fabrication and working mechanism is displayed in Fig. 5D. The inclusion of MXene improved the conductivity and electrocatalytic activity, while CeO_2 imparted antimicrobial functionality to the designed hydrogel. In addition, the hydrogel forms a hydration layer on the sensor surface, which resists biofouling and improves its real-time functionality. The sensor retained its electrochemical activity after repeated bending deformations, indicating high mechanical stability. Further, the sensor was validated in human sweat samples, showing results closely matching those obtained via the ELISA method. Similarly, Wang and team reported the use of bimetallic NPs (Au, Pd) decorated MXene-GR nanocomposite for the simultaneous sensing of DA, AA, and UA [62]. Although the sensor can effectively quantify multiple analytes, its analytical performance is considerably lower than that of the CeO_2-decorated MXene sensor.

Wang and colleagues reported a flexible DA sensor based on S, N co-doped sodium titanium layered oxide (NTLO) [63]. The fabrication process began with the synthesis of SiO_2 nanospheres, followed by coating with titanium hydroxide. This composite then underwent hydrothermal treatment to form a nano-urchin-like precursor. The precursor was subsequently annealed and deposited onto a PET substrate to obtain the desired sensor. Here, S and N doping was employed to reduce the bandgap and enhance the electrical conductivity and adsorption capability of NTLO. The sensor was further validated in artificial sweat and human serum samples, confirming its strong potential for practical applications.

Recently, Chen et al. developed a microsensor for the dynamic monitoring of DA in rat brains using a CFE modified with poly(tannic acid) (pTA), PEDOT, and ERGO [64]. The incorporation of PEDOT-ERGO enhanced the electrocatalytic activity, while pTA improved selectivity by inhibiting non-specific adsorption on the sensor surface. This sensor was successfully implanted into the striatum of the rat brain, enabling real-time quantification of dynamic DA concentrations. Compared to the G-PEDOT/LIG sensor [53], this sensor demonstrated

higher sensitivity, a lower detection limit, and a broader linear range, which could be attributed to the incorporation of ERGO into the PEDOT network. In a similar study, an inflammation-free implant was developed for in vivo DA sensing using a CFE modified with an N-doped carbon-supported iron (Fe/N-C) single-atom catalyst (SAC) [65]. The sensor exhibited excellent electrocatalytic activity toward DA in phosphate buffer saline (PBS) and artificial CSF. When applied to in vivo DA monitoring in rat brains, the sensor produced a quantifiable signal in response to the stimulated DA release. Additionally, the SAC mimicked the activity of antioxidative enzymes, helping to mitigate reactive oxygen species (ROS) generated during implantation and thereby promoting an inflammation-free integration into neural tissue. Table 2 summarizes the analytical performances of various flexible, wearable, and implantable DA sensors.

2.2.2. *Epinephrine*

Epinephrine (EP), also known as adrenaline, is both a hormone and NT released by the adrenal glands [73]. In humans, EP concentrations in bodily fluids typically range from 15 nM to 40 μM. As the primary NT of the sympathetic nervous system, EP triggers the instinctive "fight or flight" or the acute stress response, making it a valuable biomarker for stress physiology in mammals. Beyond its role in stress responses, EP is associated with various health conditions, including Parkinson's disease, heart attacks, and panic disorders. It also facilitates the mobilization of stored energy, such as ATP, to help the body respond effectively to stressful situations. Abnormal EP levels are often linked to anxiety, depression, hypertension, and sleep disorders, serving as potential diagnostic biomarkers. Additionally, EP is widely used as a medication to treat various life-threatening conditions such as cardiac arrest, asthma, and anaphylaxis. Therefore, the effective detection and monitoring of EP are crucial for understanding neurological health and improving clinical outcomes in various medical treatments [74].

Dhanjai and the team developed a non-enzymatic and cost-effective biomimetic EP sensor using a layer-by-layer (LBL) assembly approach [73]. The sensor featured a PDMS substrate, with the first layer composed of cellulose nanocrystal (CNC)-CNT nanofilms, followed by a second layer of EP-imprinted poly(aniline/phenylboronic acid) (PANI/PBA). The PDMS substrate provided flexibility, while CNC-CNT enhanced the sensitivity. The fabricated sensor demonstrated remarkable performance toward EP detection, both in standard solutions and zebrafish brain samples. In another work, a flexible, textile-based biosensor was developed for EP detection using RGO/AgNPs nanocomposite [74]. The RGO and AgNPs were synthesized via an advanced electron-beam irradiation technique, which was an efficient, eco-friendly, and easily scalable approach. Using a pad-dry-cure method, the nanocomposite was coated over precleaned cotton and polyester fabrics. Each fabric was dipped in the solution, dried, and cured at 120 °C for 3 min, and this process was repeated ten times. Under optimized conditions, both sensors showed comparable linear ranges, while polyester-based sensors exhibited lower LOD than cotton-based sensors. Similarly, Ibáñez-Redín and team utilized an electrochemically reduced graphene oxide (ERGO)-carbon black (CB) nanocomposite deposited

Table 2
Analytical performances of various DA sensors.

Sensors	Substrates	Types	Linear range (μM)	LOD (nM)	Sensitivity (μA μM^{-1} cm^{-2})	Techniques	Real samples	Ref.
f-SWCNT	PEN	Flexible	0.1–10	100	–	CV	–	[50]
Oxide/SWCNT	PEN	Flexible	0.05–0.25	50	–	DPV	–	[51]
S-CNTFs	Cotton fabric	Wearable	1–50	–	103.91	DPV	–	[52]
G-PEDOT:PSS/LIG	Kapton film	Flexible	0.5–5	567	–	CV	–	[53]
G-PANI/LIG				408	–	CV	–	
AuNPs-N-CNRs	PET	Flexible	0.02–700	7	0.60	DPV	Human serum	[54]
CS-GO-Fe_3O_4/NF	PMMA filled with graphite /paraffin oil	Wearable	0.66–90; 3–32	90	0.314*	SWV	Phantom gel and artificial ISF	[55]
			1.3–10; 3–40	600	0.015*	AMP		
ZnO/Au	PDMS	Wearable	1–100	–	7.65*	CV	–	[56]
RGO/PPY/GR-NF	Cotton@PET	Wearable	1×10^{-3}–10	1	65.2#	AMP	Artificial and real sweat	[57]
RGO/PPY/NF			1×10^{-3}–500	1	46.8#			
RGO/SS	Stainless steel filaments	Flexible	1–1000	50	–	DPV	–	[59]
CuNi-MOF@RGO	Polyimide	Wearable	1–500	–	0.019	AMP	–	[60]
MXene/CeO_2 NR/AAHG	SPE	Flexible	0.05–300	17	–	AMP	Artificial and real sweat	[61]
Au,Pd-MXene-LSG	Polyimide	Flexible	12–240	130	–	DPV	Human urine	[62]
S,N-NTLO	PET	Flexible	0.4–80	60	–	AMP	Artificial sweat and human serum	[63]
PEDOT-ERGO/pTA	Carbon fiber	Implantable	0.02–0.5; 0.5–20	9.2	1.1×10^{-3}* & 3.7×10^{-4}*	AMP	Rat brain	[64]
Fe/N-Carbon SAC	Carbon fiber	Implantable	0–25	–	0.085*	AMP	Artificial CSF and Rat brain	[65]
AuNPs-RGO-ITO	PET	Flexible	0.1–20	75	6.02	SWV	Real and artificial urine	[66]
PtNPs-RGO-ITO			0.1–10	62	7.19		Artificial urine	
Acid-oxidized CC	Carbon cloth	Flexible	0.1–104.5	10	9.32	LSV	Artificial urine	[67]
α-Fe_2O_3-acid treated-CC	Carbon cloth	Flexible	7.4×10^{-2}–113	50	0.2	AMP	–	[68]
SnO_2/conductive-CY	Carbon yarn	Flexible	0.01–150	53	0.58*	DPV	–	[69]
N,P-mesoporous carbon/CC	Carbon cloth	Flexible	2–200	600	7.94*	DPV	Human serum	[70]
MWCNT-SPE	Acetate sheet	Flexible	5–500	870	–	AMP	–	[71]
MWCNT/PEI/SSB	Sulfonated fiber	Flexible	1–650	62	–	DPV	Human serum and injection solution	[72]

AAHG – Amyloid albumin hydrogels; CC – Carbon cloth; CNR – Carbon nanorods; CS – chitosan; CY – Carbon yarn; ITO – Indium tin oxide; LIG – Laser-induced graphene; LSG – Laser scribed graphene; MOF – Metal organic framework; NF – Nafion; NTLO – Sodium titanium layered oxide; PANI – Polyaniline; PEDOT – Poly (3,4-ethylenedioxythiophene); PEI – Polyethyleneimine; PEN – Poly(ethylene naphthalene); PET – Polyethylene terephthalate; PPY – Polypyrrole; pTA – Poly(tannic acid); RGO – Reduced graphene oxide; SAC – Single atom catalyst; S-CNTFs – Spindle shaped carbon nanotube fibers; SSB – Sulfonated poly(styrene-butadiene) flexible fiber membrane. *μA μM^{-1} #mV/dec.

onto a screen-printed carbon electrode (SPCE) for the detection of EP, along with DA and paracetamol (PA) [75]. The nanocomposite was prepared by dispersing CB in a GO solution, which improved dispersion stability and minimized CB agglomeration without requiring surfactants. The resulting composite was deposited onto the SPCE, and the GO was reduced electrochemically via potential cycling. The fabrication methodology was both economical and environmentally friendly. Electrochemical investigations revealed that the sensor exhibited superior electrocatalytic activity, broad linear ranges, low detection limits, and high sensitivity for all three analytes. Comparing the structure–activity relationship of the RGO/AgNPs-based textile biosensor [74] with this work highlights how nanocomposite design and substrate choice influence sensitivity, selectivity, and wearability. Electron beam irradiation of the textile platform produced a highly conductive, porous, and flexible 3D network that combines RGO's large surface area and π–π electron transfer with the catalytic activity of AgNPs, resulting in enhanced sensitivity and low detection limits for adrenaline while maintaining breathability and mechanical flexibility for wearable use. In contrast, the interaction between RGO's conductivity and CB's defect-rich surface creates numerous active sites, reducing charge transfer resistance and enabling reliable electrochemical detection of multiple analytes (DA, EP & PA). However, this configuration offers less intrinsic flexibility and integration potential compared to the textile platform. Thus, while the textile sensor leverages a 3D hierarchical RGO/AgNPs network to maximize catalytic surface area and conformability for continuous monitoring, the ERGO–CB emphasizes composite synergy for stable, low-cost, multiplexed detection in disposable platforms, demonstrating how substrate dimensionality and nanomaterial composition directly govern sensor performance and application.

In another study, Andreotti et al. developed a flexible, economical, eco-friendly, and disposable sensor using sustainable material and inexpensive conductive ink for the detection of EP, STN and hydroquinone [76]. The conductive ink was prepared by mixing nail polish (NP) and graphite powder (GP) in a 52:48 ratio and the substrate was fabricated from recycled PET obtained from used PET bottles. The obtained GP-NP/PET sensor exhibited excellent electrocatalytic activity toward EP and STN with good selectivity. In another work, a flexible microelectrode was fabricated for the selective sensing of EP and 2-aminoadenosine (AAD) using a Cu/CuO-vertical graphene (VG) hybrid structure [77]. To prepare the Cu/CuO-VG sensor, Ta wires were polished, cleaned, and coated with a saturated $CuSO_4$ solution, then pyrolyzed in a CVD chamber to form Cu/CuO. Subsequently, VG was grown on the Cu/CuO surface by applying a DC bias at 950 °C in a methane and hydrogen atmosphere (Fig. 6A). The synergistic effects of Cu/CuO NPs and VG contributed to an enhanced sensitivity due to efficient electron transport and large ion adsorption capacity. The sensor was capable of detecting EP and AAD across a wide pH range (5.0–9.0) and concentration range and successfully quantified these analytes in human urine and blood samples (Fig. 6B).

Recently, Mugo and coworkers developed a MIP-based sensor for the selective detection of EP, lactate, and cortisol in human sweat [78]. For the fabrication of the EP sensor, a mixture of aniline, PBA, AuNPs, and EP was drop-casted onto a SPCE and polymerized on ice for one hour. After polymerization, the template molecules were removed by potential cycling in neutral PBS. The sensor exhibited excellent electrocatalytic activity toward EP and was further validated using human sweat. Sweat samples collected from the eyebrows were spiked into PBS droplets, demonstrating reliable and reproducible performance. The same group also developed a low-cost, MIP-based microneedle biosensor for the non-invasive detection of EP, DA, lactate, and pH in human sweat [79]. The sensor was fabricated using an LBL assembly method comprising four distinct layers. The base layer was a PDMS microneedle substrate, followed by a PDMS/CNT/CNC gel layer to enhance electrical conductivity. The third layer, PANI/CNT/CNC/AgNPs composite, was attached using a silylating agent and electrodeposited via amperometry. The fourth and final sensing layer consisted of a prepolymer mixture comprising of aniline, PBA, AuNPs, and EP, homogenized and drop-cast onto the microneedle array to form the MIP layer. After polymerization, the template molecules were electrochemically eluted and assembled with an RE and CE. The Ag/AgCl RE was fabricated by applying AgNPs to acetate paper, while the CNT/CNC-based CE was prepared similarly. The final sensor patch was found to effectively detect the target analytes within 2 min, demonstrating high selectivity and reproducibility across multiple measurements. The sensor's performance was successfully validated through the detection of pH, EP, DA, and lactate in human sweat, highlighting its potential as a wearable and point-of-need diagnostic platform for sweat analysis.

Compared to the flexible capacitive adrenaline sensor [73] developed by the same group, this sensor features a high surface area and selective binding cavities that enable dielectric modulation and ultralow detection limits but exhibits diffusion-limited response kinetics within the polymer. The MIP-modified SPCE [78] employs a simple, low-cost disposable carbon substrate with an electroactive MIP, allowing fast, scalable, and direct redox-based detection of sweat metabolites, albeit with lower surface area and sensitivity compared to nanostructured supports. In contrast, the microneedle MIP sensor [79] integrates 3D microelectrode structures with MIP functionalization, offering increased interfacial area, improved mass transport, and minimally invasive access to sweat or interstitial fluid, enabling rapid, multiplexed electrochemical measurements with higher fidelity in real samples. Overall,

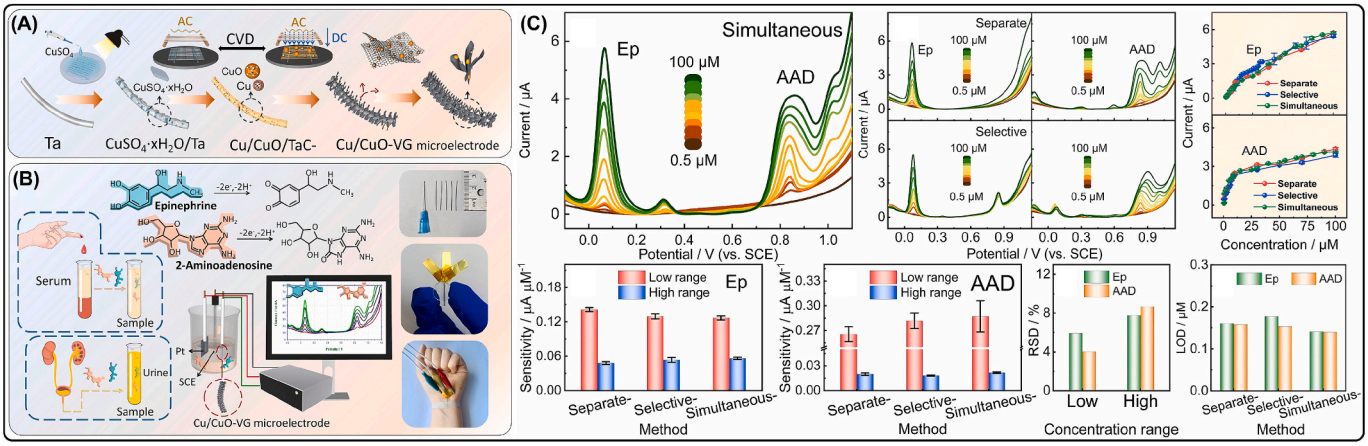

Fig. 6. (A) Graphical representation of the stepwise fabrication process of the Cu/CuO-VG sensor. (B) Electrocatalytic mechanism for EP and AAD, along with photographs of the Cu/CuO-VG sensor and its real-time applications (C) DPVs of the Cu/CuO-VG sensor for the individual, selective, and simultaneous detection of EP and AAD, along with corresponding calibration plots. Reproduced with permission from [77].

these examples demonstrate that nanostructured capacitive interfaces enhance sensitivity, planar SPCEs favor manufacturability and disposability, and microneedle architectures optimize transport and multiplexing, illustrating that electrode morphology and recognition layer design directly govern sensor performance in wearable and implantable applications.

2.2.3. Norepinephrine

Norepinephrine (NE) is an important catecholamine NT in the mammalian CNS. It plays a key role in learning, stress response, mood regulation, arousal, attention, and memory. Noradrenergic neurons are thought to respond specifically to perceived failures, potentially contributing to behaviors such as early quitting. Through its widespread influence, NE supports numerous physiological processes, helping organisms to adapt themselves to the constantly changing internal and external environments. As an excitatory agent, NE induces typical physiological responses such as increased breathing rate, heightened alertness, elevated blood pressure, and accelerated heart rate. Abnormal NE levels have been associated with a variety of disorders, including depression, anxiety, migraine, multiple sclerosis, ganglionic neuronal tumors, paraganglioma, and Parkinson's disease. Clinically, NE is also administered as a therapeutic agent in the treatment of several conditions, including organic heart disease, hypertension, myocardial infarction, and bronchial asthma [80,81].

Ji and colleagues developed a smartphone-integrated electrochemical sensing system using flexible screen-printed graphene electrodes (SPGE) for sensitive detection of NE [80]. The system comprises a smartphone with a custom Android application for device control, data processing, and result display; a coin-sized detector performing SWV; and the SPGE sensor for analyte detection. The SPGE was fabricated by screen-printing the graphene and Ag/AgCl inks onto a PET substrate, followed by oven drying, where the WE and CE used graphene ink, and the RE and conductive traces used Ag/AgCl ink. The sensor achieved NE quantification with a detection time of 12 s and a response time of 4 s, benefiting from high electron mobility and a moderate electroactive surface area that enables sensitive detection with minimal background interference. Key advantages of the system include miniaturization, easy integration with smartphone electronics, reproducibility from screen printing, rapid voltammetric PoC testing, and affordability. Its internet connectivity further supports eHealth tracking and mHealth applications. However, the platform has limited capacity for surface modification and biochemical enrichment.

In another study, a hydrogel-based electrochemical sensor was developed for assessing cognitive disorders via urinary NE detection [81]. The hydrogel consisting of titanium dioxide sol, MXene, polyvinyl alcohol (PVA), and GO was deposited onto a custom-made SPCE, and dried using a freeze-thaw method. MXene was chosen for its excellent electrical conductivity and hydrophilic surface, while TiO_2 NPs enhanced stability and minimized MXene agglomeration. PVA provided biocompatibility, along with water retention, and GO contributed to the nano-filling and cross-linking properties. The resulting 3D nanostructured composite offered a large electroactive interface and improved mass transport, achieving high sensitivity and low detection limits in complex biological fluids such as urine. The hydrogel's biocompatibility and retention capabilities also facilitated analyte preconcentration, enhancing reliability for clinical neurological screening. The sensor successfully quantified NE in human urine via offline measurements using a panty liner, showing excellent recoveries validated against HPLC-UV analysis. This work advances the development of wearable, point-of-care diagnostic tools for NE detection.

2.2.4. Serotonin

5-Hydroxytryptamine, commonly known as serotonin (STN), is a monoamine NT that plays a key role in regulating various physiological processes. STN is crucial for a wide range of brain functions, including cognition, emotional regulation, and social behavior. Its release occurs over multiple time scales: a rapid, short-term phasic release (milliseconds to seconds) triggered by neuronal firing in response to stimuli, and a slower tonic release (lasting seconds to minutes). Alterations in these release patterns can result in abnormal neurological functions and behavioral changes. The normal concentration of STN in human blood ranges from 0.6 to 1.6 μM. Deficiencies in the serotonergic system have been associated with impulse control disorders and numerous mental health conditions, including Alzheimer's disease, autism, intellectual disabilities, sleep disorders, anxiety, and depression. Conversely, abnormally elevated levels of STN can lead to carcinoid syndrome [82,83]. Therefore, accurate detection and monitoring of STN concentration in blood and other biological fluids are critically important for clinical and diagnostic applications.

Guntupalli and the team fabricated a porous hybrid film composed of AuNPs and metallic SWCNT using an ambient filtration method for the detection of STN and DA [84]. The porous films were formed via vacuum-assisted filtration of an m-SWCNT solution onto mixed cellulose ester filter paper, followed by filtration of citrate-capped AuNPs at controlled flow rates. This straightforward method yielded highly conductive, porous, and thin films that demonstrated rapid electron transfer and exceptional electrocatalytic performance–comparable to commercially available gold films or electrodeposited gold films. The flexible sensor effectively quantified both analytes with high selectivity. Owing to its larger electroactive surface area, the sensor exhibited excellent sensitivity. This novel fabrication approach is not only scalable and cost-effective but also adaptable for rapid film production and transfer onto other flexible substrates. Another flexible electrode platform featuring a WS_2/GR heterostructure on polyimide (WGP) was designed for the selective detection of STN [85]. The WGP was directly fabricated on a flexible PI substrate using PE-CVD, as shown in Fig. 7A. This fabrication method enabled the uniform and scalable formation of WS_2/GR heterostructures, where GR provided excellent electrical conductivity and WS_2 offered numerous electrochemically active sites. The sensor exhibited well-resolved voltammetric signals for STN with a potential separation of 188 mV. Its practical utility was demonstrated through successful testing in cerebrospinal fluid (CSF), yielding satisfactory recovery rates and confirming its potential for real-world biomedical applications.

Chavan and coworkers constructed an STN sensor using conformationally flexible dimeric-STN self-assembled on a gold surface [86], and the stepwise fabrication process is illustrated in Fig. 7B. This was the first report of this kind for STN detection, and the proposed method proved to be robust, economical, and highly sensitive. Ko et al. developed a hybrid interface using ERGO-PEDOT:PSS/NF for the simultaneous sensing of STN and DA [87]. Initially, GO was electrophoretically deposited onto an Au-coated PI substrate and subsequently reduced to ERGO. PEDOT:PSS was then coated via electropolymerization and finally covered with an NF layer (Fig. 7C). The hybrid design of electrodeposited ERGO–PEDOT:PSS/NF features multiple layers: RGO offers high surface area and conductivity, PEDOT:PSS provides electrochemical stability and efficient charge transfer, and NF acts as a selective ion-exchange barrier. This configuration enables the simultaneous detection of neurotransmitters with high sensitivity and selectivity, although it relies on a flexible Au substrate, which limits its long-term in vivo applications.

In another work, a wearable microneedle patch was designed for the real-time continuous electrochemical sensing of STN using an RGO/Ag-modified carbon paste microelectrode [88]. The microneedle patch was fabricated from PMMA and coated with the as-prepared RGO/Ag nanocomposite. The wearable RGO/Ag/CS microneedle sensor exhibits a composite structure–activity relationship, where RGO contributes to conductivity and strength, Ag serves as catalytic sites, and CS ensures biocompatibility and structural integrity. Its microneedle design enhances analyte access for real-time, minimally invasive monitoring. The sensor effectively quantified STN in artificial ISF and its performance was validated in a skin-mimicking model, confirming its potential for

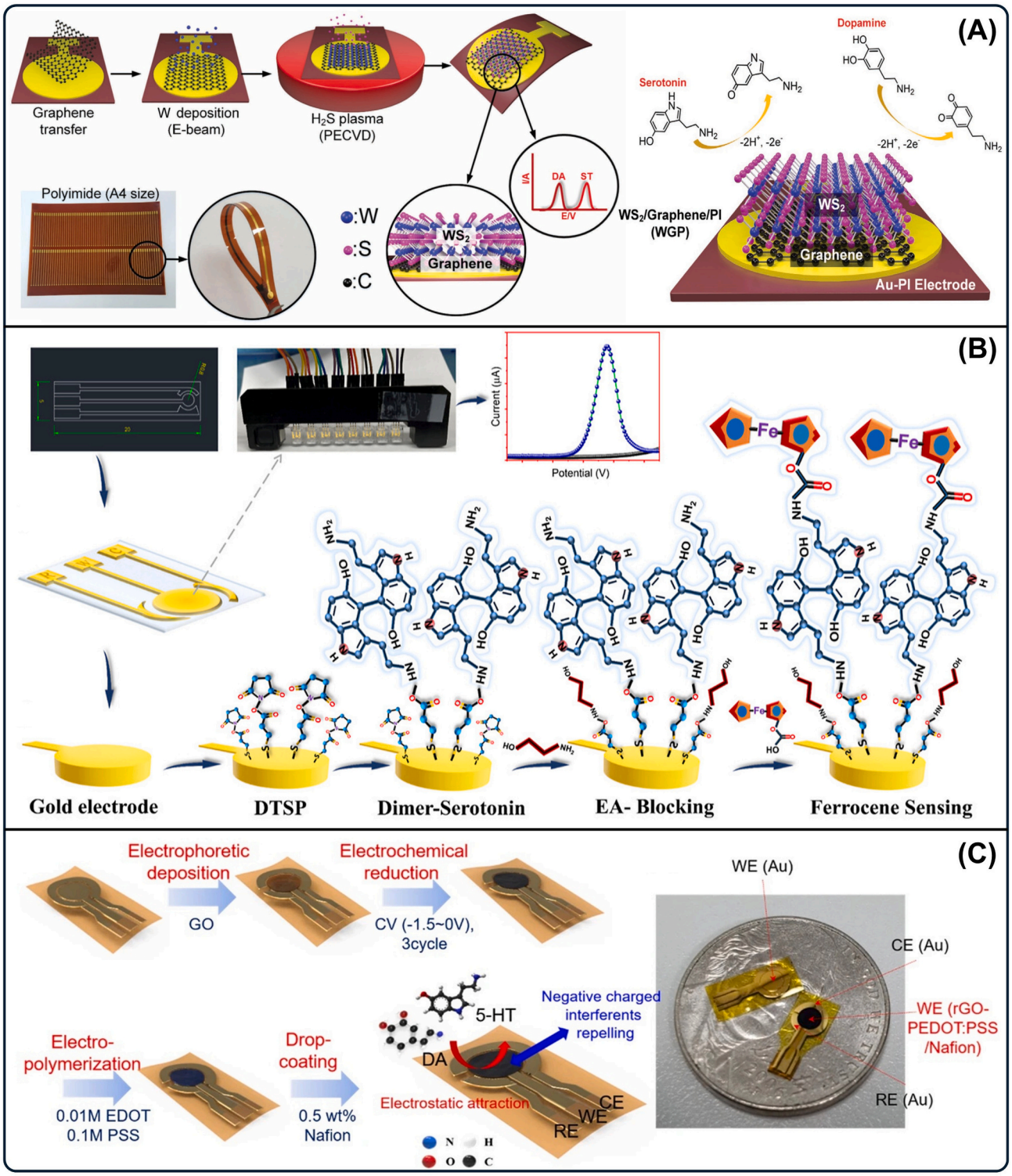

Fig. 7. Graphical illustration of the stepwise fabrication of (A) the WGP sensor and its electrocatalytic activity toward DA and STN. Reproduced with permission from [85]. (B) Dimer-serotonin sensor. Reproduced with permission from [86]. (C) ERGO-PEDOT:PSS/NF sensor. Reproduced with permission from [87].

real-time, non-invasive STN monitoring. Recently, Castagnola and co-workers constructed implantable microelectrode arrays (MEAs) using PEDOT/CNT modified GC for in vivo sensing of tonic STN [89]. The MEAs were batch-fabricated on a flexible SU-8 substrate, providing a stable and biocompatible interface with neural tissue. The sensor array combined a durable, conductive GC base with PEDOT for stability and CNTs to increase surface area and enable rapid electron transfer, supporting long-term, stable in vivo serotonin sensing. It successfully quantified basal STN levels at multiple sites within the CA2 region of the hippocampus in both awake and anesthetized mice. Post-implantation, the sensor remained functional for up to one week and exhibited reduced inflammatory response and tissue damage compared to commercial probes. The authors claimed that this MEA was the first flexible, implantable sensor designed for chronic, multi-site, in vivo detection of tonic STN.

Another implantable sensor was developed for the simultaneous

sensing of DA and STN in a freely moving crayfish [90]. The sensor was fabricated by dip-coating a CFE with an NF/CNT solution and connecting it to a miniaturized potentiostat (Fig. 8A), which was then implanted into the pericardial cavity via a small incision. Upon injection of STN and DA into the ventral sinus cavity, the sensor successfully quantified both NTs in real time (Fig. 8D). This miniaturized design, with surface electrochemical modifications, balances conductivity, sensitivity, and minimal invasiveness, enabling real-time neurochemical monitoring. Moreover, it demonstrates the sensor's effectiveness for multi-analyte detection in freely moving organisms. Overall, these studies [87–90] illustrate how optimizing structure–activity relationships through layered composites for selectivity, nanocomposites for wearability, sturdy conductive substrates for chronic use, or miniaturized electrodes for minimally invasive in vivo sensing can enhance sensor performance across diverse applications. Table 3 summarizes the analytical performances of other monoamine NT sensors. As per the Scopus literature survey, there are currently no reported studies on flexible, wearable, or implantable sensors for monoamine NTs beyond those discussed above. This gap presents significant opportunities for researchers to develop and explore innovative approaches for the flexible, wearable, and implantable sensing of additional monoamine NTs.

2.3. Gasotransmitters

Gasotransmitters are a critical class of NTs consisting of small gaseous molecules produced endogenously to accomplish various signaling functions in the living body, from microbial systems to mammalian physiology. Some of the well-known gasotransmitters include nitric oxide, carbon monoxide, and hydrogen sulfide. Until recent findings revealed the physiological relevance of these gasotransmitters, they have been considered as toxic and poisonous substances. Due to their small size and slight polarity, gasotransmitters can diffuse freely through both aqueous and lipid environments. Their unique chemical properties make them versatile and ubiquitous signaling agents. Gasotransmitters exhibit a biphasic role in physiology—at low concentrations, they exert beneficial effects, while at

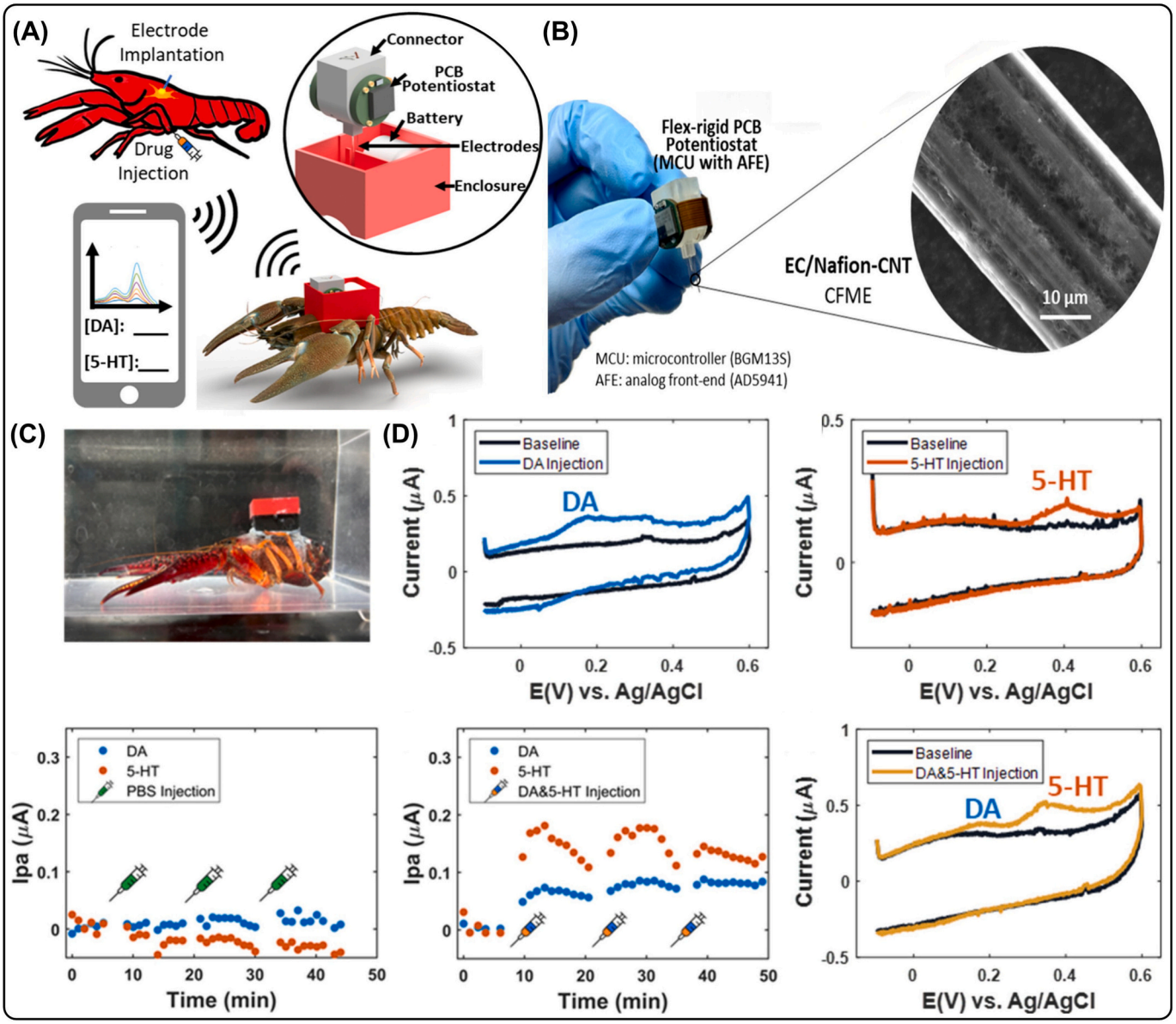

Fig. 8. (A) Graphical representation of the crayfish-implanted device with wireless detection capabilities (B) Actual image of the miniaturized potentiostat and SEM image of the NF/CNT/CFE sensor (C) Photograph of the implanted crayfish. (D) Electrochemical response showing individual and simultaneous detection of baseline and injected concentrations of DA and STN. Reproduced with permission from [90].

Table 3
Analytical performances of epinephrine, norepinephrine and serotonin sensors.

Sensors	Substrates	Types	Analyte	Linear range (μM)	LOD (nM)	Sensitivity (μA μM^{-1})	Techniques	Real samples	Ref.
PANI/PBA-CNC/ CNT	PDMS	Flexible	EP	1×10^{-3}–100	1.0	–	CV	Zebra fish	[73]
RGO/AgNPs	Polyester Cotton	Flexible	EP	1–30 5–40	3.05 9.73	–	SWV	–	[74]
CB-ERGO/SPCE	PET	Flexible	EP DA	10–100 5–29	1.8×10^3 410	0.12 1.50	SWV	–	[75]
NP-GP	PET	Flexible	EP STN	5–100 1–50	300 100	–	DPV	Synthetic urine	[76]
Cu/CuO-VG	Ta filaments	Flexible	EP	0.5–11 & 11–100	160	–	DPV	Synthetic urine and serum	[77]
PANI-co-PBA/AuNPs/ SPCE	PET	Wearable	EP EP	5.6×10^{-4}–0.014 5.6×10^{-4}–0.02	8.2 0.6	– 9.4×10^3	CV DPV	Human sweat	[78]
MIP-CNC/CNT /PDMS	PDMS	Wearable	EP DA	0.304–121 0–0.763	0.7 2.11	–	CV	Human sweat	[79]
GR/SPGE	PET	Flexible	NE	1–30	265	–	SWV	–	[80]
TiO_2/MXene-PVA/ GO/SPCE	PET	Flexible	NE	0.01– 1 &1–60	6.0	–	AMP	Urine samples	[81]
WS_2/GR	Polyimide	Flexible	STN DA	0.249–9.9 1.24–13.37	–	–	DPV	Artificial cerebrospinal fluid	[85]
DTSP-AuE	–	Flexible	STN	0.01–0.4	0.9	20.0	DPV	Human serum	[86]
ERGO-PEDOT:PSS/ NF	Au-coated Polyimide	Flexible	STN DA	0.05–50 0.5–75	160 170	– –	DPV	Human serum	[87]
RGO/Ag/CS	PMMA	Wearable	STN	3–21 & 6–60	900	1.01×10^{-2} & 2.32×10^{-2}	CA	Artificial interstitial fluid	[88]
PEDOT/CNT	Glassy carbon	Implantable	STN	0.05–1	–	–	SWV	Mouse hippocampus	[89]
NF/CNT	Carbon fiber	Implantable	STN DA	0.1–1 0.1–1.5	59.3 85.1	0.25 0.13	DPV	Crayfish	[90]

AuE – Gold electrode; CB – Carbon black; CNC – Cellulose nanocrystal; CNT – Carbon nanotubes; CS – Chitosan; DTSP - Dithiobis (succinimidyl) propionate; GO – Graphene oxide; GP – Graphite powder; GR – Graphene; NF – Nafion; NP – Nail polish; PANI – Polyaniline; PBA – Phenylboronic acid; PVA – Polyvinyl alcohol; RGO – Reduced graphene oxide; SPGE – Screen printed graphene electrode VG – Vertical graphene.

higher concentrations, they can become toxic and potentially lethal [91].

2.3.1. Nitric oxide

Nitric oxide (NO) is a naturally occurring free radical involved in numerous physiological processes, including blood pressure regulation, tissue regeneration, synaptic communication, vasodilation, and immune response, despite its high chemical reactivity and short half-life in biological systems. It is recognized as an endothelium-derived relaxing factor (EDRF) and functions as a free radical signaling molecule that also inhibits platelet aggregation. Abnormal levels of NO have been linked to a range of clinical conditions, including sepsis, asthma, neurovirulence, inflammation, and cancer progression [92,93]. As a result, the real-time detection in biofluids is of significant interest in both pathological studies and clinical research.

A highly selective electrochemical sensor was developed for the in situ detection of NO using a multicomponent core@cage structure composed of Cu_2O@$FePO_4$ [94]. In this design, the outer shell of iron phosphate provided an enhanced electrocatalytic activity, while the inner core of cuprous oxide facilitated faster electron shuttling. The synergistic interaction between the two components significantly improved the overall sensor performance. The sensor exhibited a rapid response time of 0.8 s and an impressive detection limit of 0.45 nM. Its effectiveness was validated through the detection of NO released from cancer cells. In another study, a robust electrocatalyst consisting of nickel single atoms anchored on N-doped hollow carbon spheres (Ni SA/N-C) was developed for the electrochemical sensing of cellular NO [95]. The reaction mixture, comprising DA monomer, nickel acetate, TEOS, aqueous ammonia, and ethanol, was stirred for 12 h, followed by centrifugation and pyrolysis. After pyrolysis and etching, a hollow nitrogen-doped carbon structure with atomically dispersed nickel was obtained. The nickel atoms were coordinated with nitrogen to form highly active Ni—N_4 catalytic centers. A flexible sensor was then fabricated by depositing Ni SA/N-C onto a PDMS substrate and coating it with NF to minimize interference. Electrochemical investigation revealed that the sensor has a linear detection range of 1.8–360 nM with a LOD and sensitivity of 1.8 nM and 430.6 nA μM^{-1} cm^{-2}, respectively. The sensor maintained consistent performance even under mechanical deformation and enabled real-time NO detection in human umbilical vein endothelial cells (HUVECs) under both chemical and mechanical stimulation. Although this sensor demonstrated superior sensitivity, selectivity, and operational stability, its detection limit was higher than that of the previously reported core@cage sensor. This could be attributed to the incorporation of NF in the former, which may have compromised its lower detection capability. In another study, an implantable, biodegradable, and smartphone-integrated NO sensor was developed using a copolymer and gold nanomembrane [96]. The sensor featured a substrate made from poly(lactic acid) and poly(trimethylene carbonate) (PLA-PTMC) onto which a gold nanomembrane was deposited via magnetron sputtering, as shown in Fig. 9A. A final layer of poly (eugenol) was electrodeposited to enhance selectivity and biocompatibility. The developed PLA-PTMC provided flexibility, stretchability, and hydrolytic biodegradability, while the gold layer improved conductivity and active surface area. This sensor demonstrated a linear range of 0.01–100 μM with a LOD of 3.97 nM and a fast response time of 350 ms. It was successfully validated by detecting NO released from rat chondrocytes and organs, as well as in vivo measurements in the rabbit heart and joint cavities (Fig. 9H-K).

Another stretchable NO sensor was developed using CNT and silver nanowires (AgNWs) deposited onto a flexible PDMS substrate. The sensor exhibited good sensitivity, selectivity, and mechanical stability for NO detection, with a linear range of 10 nM – 60.94 μM and a LOD of 2.5 nM [97]. Similarly, a multifunctional 3D scaffold-based sensor was developed for real-time NO sensing using enokitake-like gold nanowires (AuNWs) and conductive carbon (C—C) coated PDMS [98]. Initially, a PDMS scaffold was formed using a sacrificial nickel foam template,

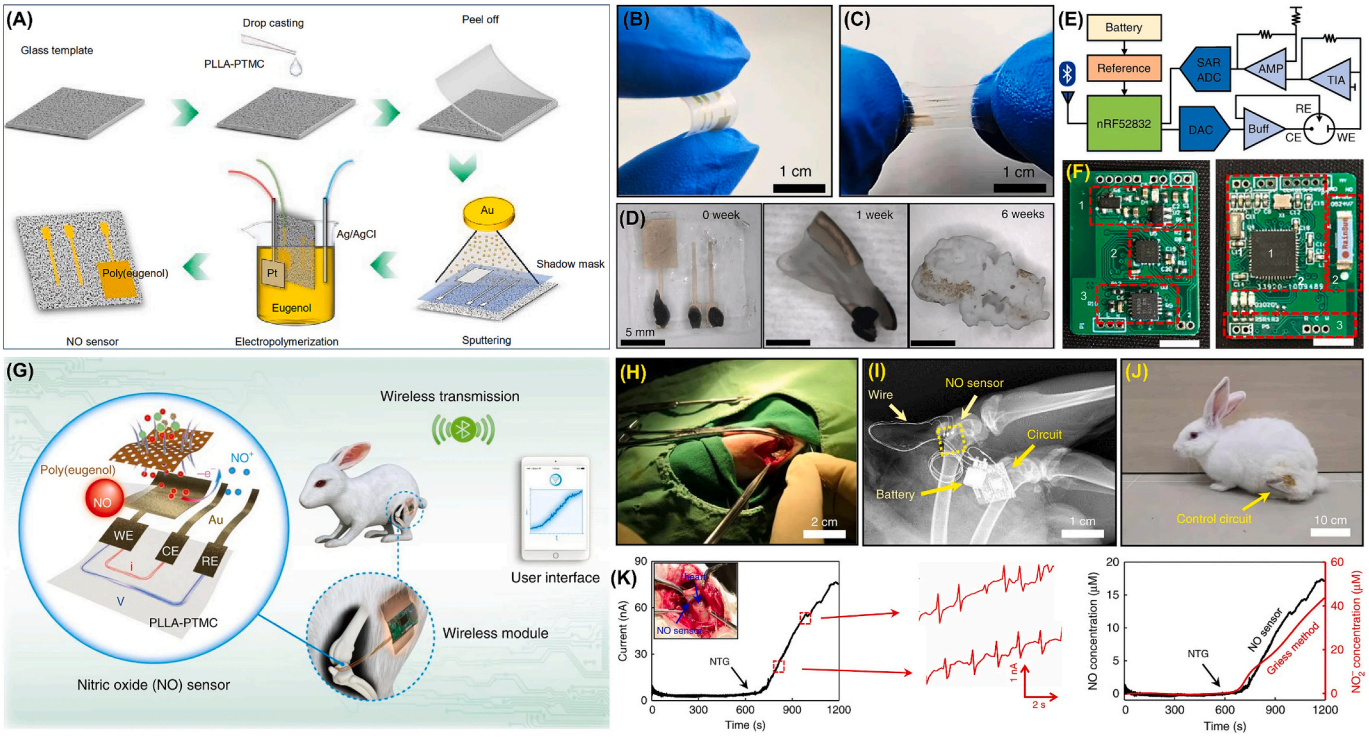

Fig. 9. (A) Illustrates the stepwise fabrication process of the NO sensor. (B, C) Photographs demonstrating the flexible and stretchable nature of the developed sensor. (D) Images of various stages of accelerated degradation of the sensor in PBS solution at 65 °C. (E) Block diagram of the electronic circuits. (F) Photographs of the actual electronic circuits. (G) Graphical illustration of the working principles of the implanted NO sensor with a user interface. (H) Surgical implantation procedure, (I) X-ray image of the implanted NO sensor and its components. (J) Photograph of the NO sensor implanted in an animal model. (K) Real-time monitoring of NO release from the heart following nitroglycerine stimulation, along with corresponding electrocardiography recordings, compared with standard Griess tests. Reproduced with permission from [96].

followed by coating with a C—C layer. AuNWs were then grown on the C-C/PDMS substrate via a seed-growth solution method, as displayed in Fig. 10A. Even though the AuNWs/C-C/PDMS sensor demonstrated excellent electrocatalytic activity and high sensitivity, their linear range (2.5 nM to 23.95 μM) and LOD (8 nM) values are poorer than those of the AgNWs-modified sensor. Furthermore, the sensor's real-time performance was validated by detecting NO released from HUVECs (Fig. 10C). More recently, a cost-effective, paper-based electrochemical NO sensor was developed using flexible butter paper modified with CC and AuNPs [99]. A three-electrode system was painted with carbon ink on butter paper, and the WE was further modified with AuNPs/CC to enhance sensing performance (Fig. 10E). The designed sensor demonstrated high sensitivity over a broad linear range of 10 nM to 0.4 mM, with an LOD of 2.35 nM. The sensor was successfully evaluated in artificial tear samples and cross-validated using the standard Griess assay. Here, the sensor incorporated with AuNPs exhibited a wider linear range and lower detection limits compared to the AuNWs-modified sensor. However, the AuNWs-based sensor was successfully applied to quantify cellular NO released during endothelial mechanotransduction.

2.3.2. *Hydrogen sulfide*

Hydrogen sulfide (H_2S), the third gasotransmitter in biological systems, belongs to the family of reactive sulfur species. It is intricately linked to a wide range of physiological and pathological processes, including inflammation, cellular signaling, neurodegenerative disorders, and hypertension. As such, accurate quantification of H_2S is critically important in clinical and biomedical research. Recently, Li and coworkers developed a stretchable and transparent H_2S sensor using CNT and AuNWs embedded in a PDMS matrix [100]. The AuNWs were first prepared and vacuum-filtered onto a filter membrane to form a uniform film. Subsequently, a dispersed CNT solution was filtered onto the AuNW layer, forming a CNT-AuNW composite film. This film was then transferred onto a semi-cured PDMS substrate and fully cured, after which the filter membrane was removed to yield the desired stretchable H_2S sensor. The sensor exhibited excellent electrocatalytic activity for H_2S oxidation, with a broad linear detection range from 5 nM - 24.9 μM and a LOD of 3 nM. Owing to its biocompatibility and mechanical flexibility, the sensor supported the direct culture of HeLa cells on its surface, enabling real-time monitoring of H_2S release under mechanical stretching and stimulation with cysteine.

Xu and the team developed a smartphone-enabled microfluidic electrochemical sensor integrated with an electroactive nanocarbon microelectrode for the sensitive and selective detection of multiple biomarkers in various biological samples [101]. The fabrication process began with an ionic liquid (IL)-assisted wet spinning of GO to obtain IL-GO, followed by the tailored growth of ZIF-67 on IL-GO fibers. Subsequent pyrolysis in the presence of melamine produced the targeted microfibers with excellent electrochemical properties. The nanocarbon microelectrode featured a bottlebrush-like structure consisting of a free-standing N, B-co-doped GR fiber stem and densely packed Co, N-co-doped CNT array bristles. This architecture significantly enhanced the mechanical and electrical properties, electroactive surface area, surface physicochemical characteristics, and electrocatalytic activity. Under optimized conditions, the sensor exhibited a dynamic linear range of 500 nM - 4.44 mM, with a LOD and sensitivity of 75 nM and 0.8 mA cm^{-2} mM^{-1}, respectively, for H_2S detection. The developed microelectrode was successfully applied for on-chip monitoring of H_2S and DA released from neuroblastoma cells, as well as for the simultaneous detection of DA, UA, and AA in body fluids. Although co-doping CNT with Co and N resulted in a wider linear range, improved sensitivity, and enabled multiplexed monitoring, its detection limit was significantly higher than that of CNT decorated with AuNWs. Recently, the same group designed a fully integrated, smartphone-compatible microfluidic electrochemical sensor for real-time monitoring of H_2S and H_2O_2

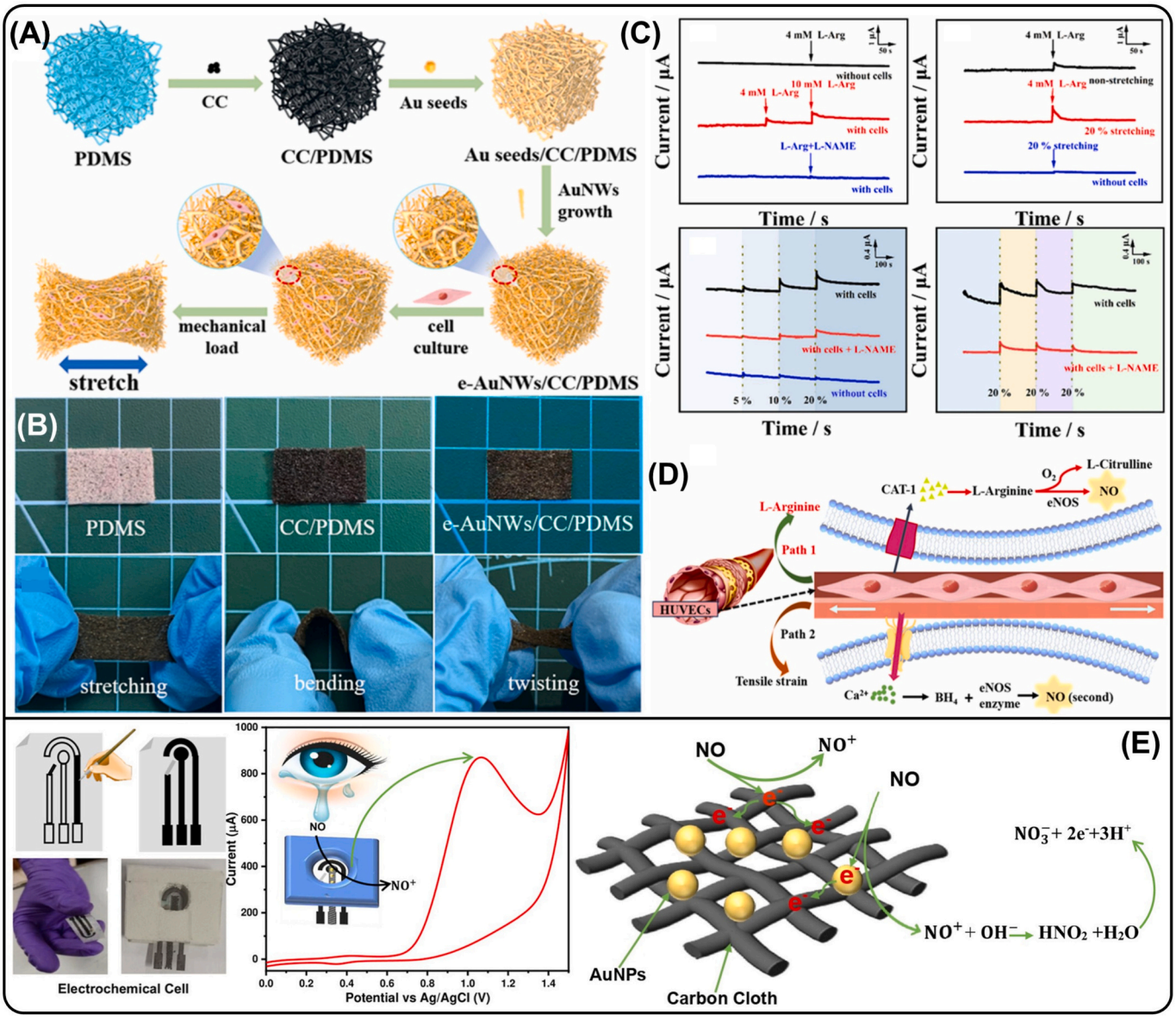

Fig. 10. (A) Graphical illustration of the fabrication steps for the AuNWs/C-C/PDMS sensor. (B) Photographs of PDMS, C-C/PDMS and the final scaffold in stretched, bent, and twisted states. (C) Amperometric response of the sensor to NO release by HUVECs. (D) Schematic representation for the cellular mechanotransduction mechanism. Reproduced with permission from [98]. (E) Schematic representation for the fabrication of a paper-based sensor, its electrocatalytic oxidation of NO, and the sensing mechanism. Reproduced with permission from [99].

secreted from biological samples [102]. The sensor was constructed by growing a nanorod-shaped RuCu-bimetallic MOF on a flexible CFE (Fig. 11). This biocompatible microelectrode was then incorporated into a wireless microfluidic chip, enabling real-time, in situ monitoring of redox signaling molecules released from live cells. The system successfully distinguished between normal and cancerous cells based on their secretion profiles of H_2S and H_2O_2. Although the nanorod-shaped bimetallic MOF sensor exhibited a wider linear range of up to 59.44 mM, its sensitivity and detection limit were significantly inferior to those of the bottlebrush-shaped Co, N co-doped CNT sensor. When applied to colorectal cancer tissues, the sensor effectively tracked biochemical changes in response to chemotherapy. The authors highlighted the potential of this platform for diagnostic and therapeutic applications in cancer management. The development of flexible and wearable H_2S, NO, and CO sensors remains an emerging technology, with only a few pioneering research groups leading progress. This presents substantial opportunities for future exploration and innovation in this promising area.

2.4. Other NTs

2.4.1. Acetylcholine

Acetylcholine (ACh) was the first NT ever discovered, identified by Otto Loewi in 1921. It is synthesized in nerve cells from acetyl coenzyme A and choline, catalyzed by the enzyme choline acetyltransferase. ACh plays a crucial role in transmitting signals from neurons to muscles, thereby enabling movement. It also facilitates communication between different regions of the brain, contributing to the key cognitive functions such as reasoning, memory, motivation, language and attention. Disruptions in ACh signaling have been linked to various neurological and psychiatric disorders, including dementia, anxiety, depression, and Alzheimer's disease [103]. Therefore, accurate quantification of ACh is highly significant in clinical diagnostics and medical research. Early sensors for ACh detection were constructed using rigid materials like

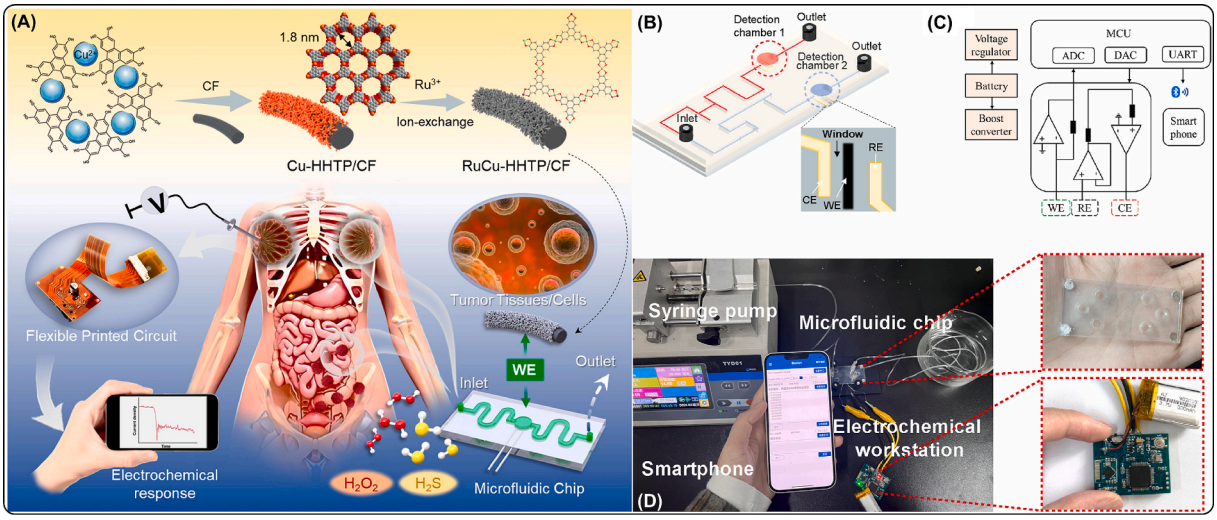

Fig. 11. (A) Graphical representation of the fabrication of the RuCu-MOF microelectrode and its application for detecting H_2S and H_2O_2 released from cancer cells and tissues using a custom-designed multichannel microfluidic chip. (B) Microfluidic device featuring a three-electrode configuration. (C) Block diagram of the electronic system. (D) Photograph of the smartphone-enabled, fully integrated electrochemical sensing platform. Reproduced with permission from [102].

silicon and metals, which often caused significant tissue damage. Recent advancements, however, have shifted toward softer, more biocompatible materials such as polyimides and parylene, minimizing harm to delicate brain tissues.

Amirghasemi and coworkers developed a flexible solid-contact sensor for the detection of ACh in tissue homogenate and brain samples [104]. The sensor was fabricated by coating cotton yarn (CY) with conductive ink and an ACh-selective membrane (Fig. 12A). The conductive ink was prepared by mixing CB with an organic polymer composed of polyvinyl chloride (PVC) and plasticizer o-NPOE in a 1:3 ratio. The ACh-selective membrane consisted of PVC, NaTFPB, calix[4] arene, and o-NPOE and was coated with ACh chloride (Fig. 12E). To insulate the sensor, a thick layer of parylene C was applied to the middle section of the thread, leaving 1 cm conductive yarn exposed at both ends. This sensor directly measured ACh by detecting changes in electrical potential at the interface where the ACh-selective membrane contacts ACh ions in the solution. The sensor was evaluated under various conditions, including sheep brain mixture, fresh brain tissue, and artificial CSF, and demonstrated reliable performance. CB provided a large active surface area, while CY contributed mechanical stability and flexibility (Fig. 12F). Owing to its compact and flexible design, the sensor minimized tissue damage during implantation. The sensor accurately measured ACh concentrations over a wide linear range in deionized water and artificial CSF. In another study, an advanced electrochemical ACh sensor was developed by modifying the carbon cloth (CC) with enhanced interfacial properties [105]. At first, the CC was electrochemically activated, followed by the electrodeposition of RGO, forming RGO/CC. Subsequently, a Cu-MOF was electrodeposited, and finally, α-MnO_2 was deposited via anodic-induced electrochemical methods to complete the desired sensor, as shown in Fig. 12G. The combination of highly conductive materials and uniform MnO_2 doping created a synergistic effect, thereby greatly enhancing the sensor performance. The sensor was successfully employed in real-time detection of ACh released from various cell lines under nifedipine stimulation.

Similarly, an ACh sensor with sub-nanomolar detection capability was developed using an intertwined copper cobaltite (CuCo) and MWCNT nanocomposite [106]. An interface-assisted technique was employed to synthesize CuCo with controlled morphology and structure. Among the different Cu:Co ratios assessed, the braided CuCo (1:20) exhibited superior electrocatalytic activity compared to the 1:2 and 1:10 combinations. This enhancement can be attributed to the improved crystallinity and braided morphology at the 1:20 ratio, which facilitated more efficient diffusion of reactive species to the electrode surface and enabled faster electron transport. The resulting CuCo was mixed with different proportions of MWCNTs to produce the sensor ink, which was then coated onto a PI substrate to fabricate the desired sensor. The sensor demonstrated excellent electrocatalytic activity toward ACh in a basic medium, achieving an LOD of 0.8 nM. The practicability of the sensor was validated using human neural cells, showing acceptable recoveries. In a recent advancement, Amirghasemi et al. developed a flexible neural probe for ACh monitoring using hydrophobic LIG modified with an ACh-selective membrane [107]. This membrane was doped with a fluorophilic cation-exchanger, which selectively permitted the passage of hydrophobic ions such as ACh to the sensor surface, thereby offering enhanced selectivity against other common ions in the brain. Compared to conventional sensors, the developed sensor demonstrated a broader linear range and a lower LOD. In an artificial CSF solution, the sensor showed a LOD of 0.38 μM with a sensitivity of 54.14 ± 1.8 mV/decade. Overall, the fluorous-phase electrode outperformed traditional sensors in terms of selectivity, sensitivity, and detection limits, paving the way for improved understanding of ACh-related brain disorders.

Upon critical analysis of the ACh reports, it is evident that the FAST device [104] serves as compelling proof of concept with an advantageous form factor but limited sensitivity. The flexible neural probe [107] advances the materials frontier by improving selectivity and stability, yet still requires bridging the gap to physiological sensitivity, kinetic resolution, and in vivo validation. When comparing the CC-based sensor [105] and the braided flexible sensor [106], the former represents a strong platform for future development if coupled with sensitivity enhancements and biological validation. In contrast, the latter holds greater immediate potential for real-time neurochemical sensing, provided its claims are validated under realistic biological conditions.

2.4.2. *Adenosine*

Adenosine (ADO), formed through ATP hydrolysis, plays a critical role in various physiological and pathological processes such as neurotransmission, trauma, inflammation, ischemia, and more. An implantable aptasensor was developed for the selective in vivo sensing of ADO using an aptamer immobilized RGO-gold nanoclusters (GNCs) modified needle-type Pt electrode [108]. The Pt electrode was first electrodeposited with RGO, followed by GNCs, then functionalized with ADO-specific aptamers, and finally coated with the redox-active indicator methylene blue (MB), as illustrated in Fig. 13A. In this setup, RGO and

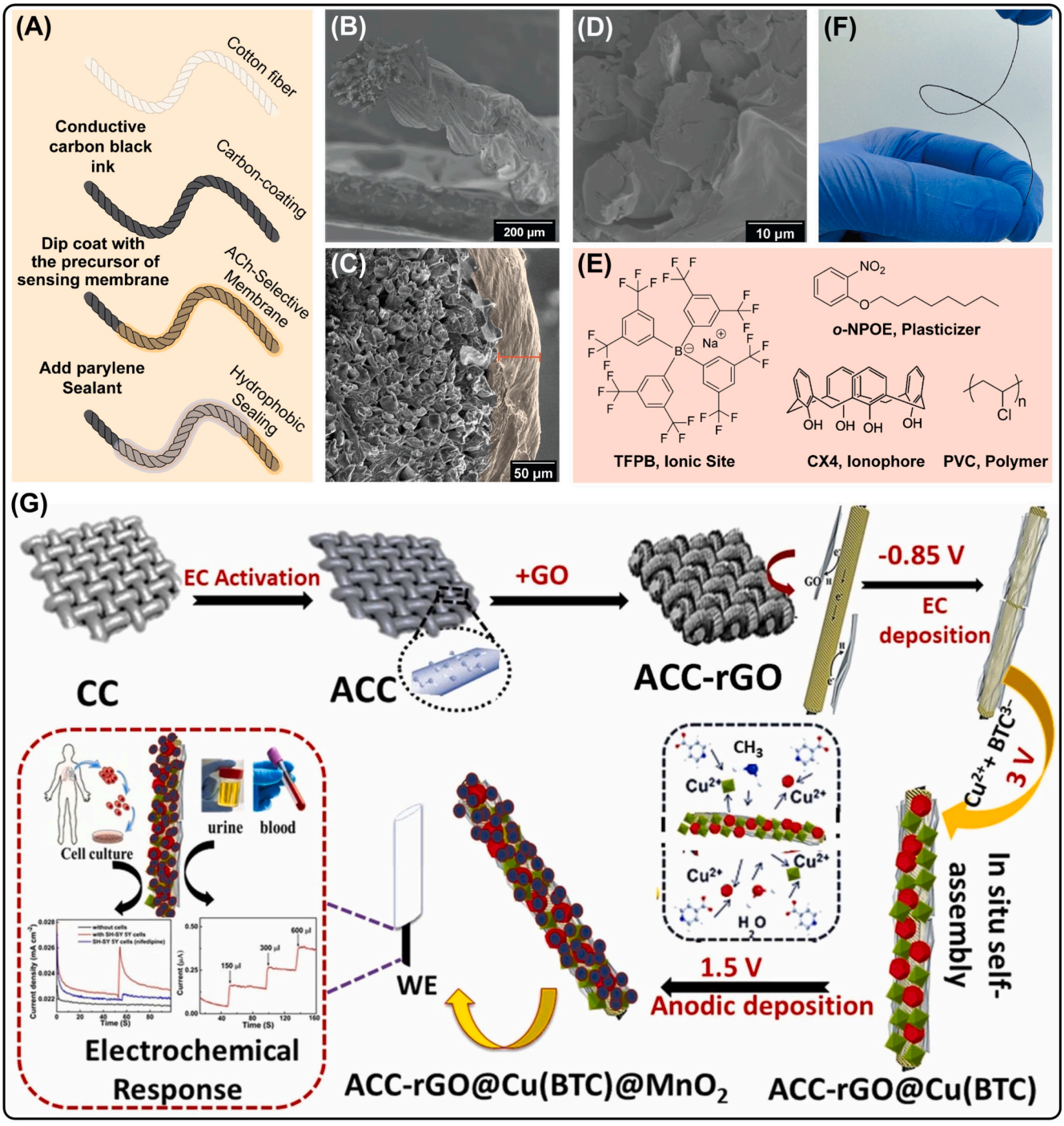

Fig. 12. (A) Scheme for the fabrication of a carbon yarn-based ACh sensor. SEM images of (B) CB-coated CY, (C) ACh-membrane coated CB/CY, and (D) Parylene-coated ACh-m/CB/CY. (E) Chemical structures of the components used in the ACh-selective membrane. (F) Photograph of carbon yarn electrode. Reproduced with permission from [104]. (G) Schematic illustration of the fabrication steps for the modified CC sensor and its electrocatalytic activity toward ACh detection. Reproduced with permission from [105].

GNCs enhanced the conductivity of the sensor, while MB served as a label to monitor target binding/cleavage events. The sensor was successfully implanted into a rat model, where it effectively monitored externally injected ADO concentrations, showing a strong correlation with expected levels. More recently, a flexible microbiosensor was developed for ADO detection, incorporating Prussian blue (PB), a permselective membrane, and a multienzyme system [109]. Initially, PB was electrodeposited onto a Pt electrode, followed by drop-coating of polyethyleneimine-modified GO mixed with a cocktail of enzymes – adenosine deaminase, xanthine oxidase, and nucleoside phosphorylase, along with genipin as a crosslinker. To enhance selectivity and reduce biofouling during in vivo applications, the sensor was further coated with electrodeposited PoPD. A schematic overview of the fabrication process is shown in Fig. 13B. When implanted into a rat model, the sensor successfully monitored ADO release induced by acupuncture stimulation, quantifying ADO levels in response to varying stimulus intensities. Here, both studies highlight the fundamental trade-offs in electrochemical biosensing, balancing sensitivity, selectivity, response

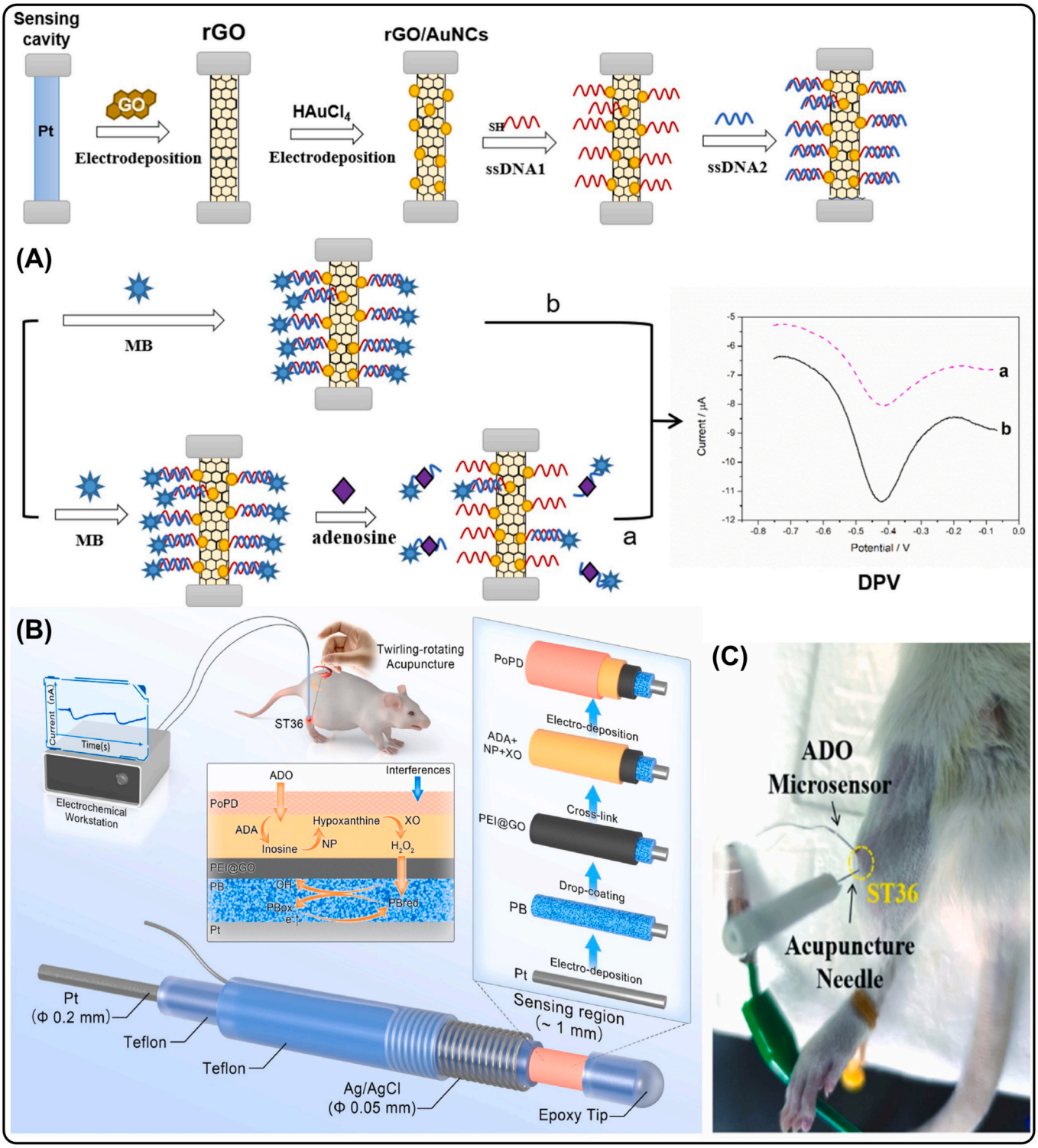

Fig. 13. (A) Schematic illustration of various steps involved in the fabrication of the ADO sensor and its electrochemical response. Reproduced with permission from [108]. (B) Graphical representation of the components of the ADO microsensor and its working mechanism. (C) Photograph showing the implantation of the ADO into a Rat's limb. Reproduced with permission from [109].

speed, and operational stability in animal models. The former demonstrates excellent specificity but suffers from limited durability, as the electrode's activity depends heavily on the integrity of molecular-scale aptamer structures. In contrast, the latter offers greater durability through a macro–nano electrode morphology that enhances binding capacity and electron transport; however, it still requires thorough validation of its long-term performance and operational stability.

2.4.3. *Neuropeptide Y*

Neuropeptide Y (NPY) is one of the most abundant neuropeptides in the CNS, synthesized in the arcuate nucleus of the hypothalamus. Belonging to the pancreatic polypeptide family, NPY engages in a variety of physiological processes, including appetite regulation, cardiovascular function, stress response, and neuroendocrine modulation. Elevated levels of NPY have been observed in patients with major

depressive disorder (MDD), a prevalent mental health condition worldwide [110]. Therefore, the development of highly sensitive NPY sensors would be of great significance for the diagnosis, treatment, and monitoring of stress-related and affective disorders.

Mintah and coworkers developed a flexible NPY sensor using a porous gold electrode modified with a thiolated self-assembled monolayer (SAM) [111]. Initially, porous gold nanostructures were deposited onto polyamide substrates and subsequently modified with the thiolated linker dithiobis-succinimidyl propionate, which facilitated antibody immobilization. Using this sensor, a PoC system was then established using a portable EmStat Pico device, which successfully quantified the spiked NPY samples. Recently, a flexible and cost-effective NPY sensor was developed using a non-conductive overhead projector (OHP) sheet modified with PPY and PEDOT-EG3 nanotubes [112]. Initially, the OHP sheets were rendered conductive by coating with PPY, followed by modification with PEDOT-EG3 to enhance selectivity and minimize non-specific binding. Antibodies were subsequently immobilized on the electrode surface via EDC/NHS coupling, resulting in the final sensor. The sensor exhibited a wide linear detection range with an ultra-low LOD and good recovery in artificial sweat samples. Overall, the OHP-based sensor demonstrates notable advances in sensitivity and cost-effective substrate design, offering improved performance and strong potential for wearable applications, thereby marking a promising step forward in electrochemical biosensor technology. Nevertheless, both NPY sensors must progress beyond controlled synthetic testing and establish reliable, long-term operation in real human sweat, with robust resistance to signal drift and performance degradation. Table 4 compares the analytical performances of various flexible, wearable, and implantable NT sensors.

3. Sensor architecture: importance and implications

Sensor architecture plays a pivotal role in defining the sensitivity, selectivity, stability, and overall performance of electrochemical devices. A well-designed architecture not only facilitates efficient electron transfer and signal transduction but also determines the adaptability of the sensor for wearable, implantable, and real-time applications. In this section, we consolidate the available literature on the fabrication of flexible, wearable, and implantable electrochemical NT sensors, with particular emphasis on the influence of sensor architecture. For better understanding and clarity, the discussion has been segregated into two categories: (i) architectures incorporating carbon nanostructures (CNSs) and (ii) those developed without CNSs.

In general, monoamine-based NT sensors (e.g., dopamine, serotonin, epinephrine) predominantly employ CNSs in their electrode designs. This can be attributed to the facile electro-oxidation of monoamines, as well as the widespread availability, low cost, large surface area, tunable functionality, and excellent adaptability of CNSs. Importantly, CNSs can synergistically combine with other nanomaterials to enhance overall sensor performance. Moreover, CNSs-based electrodes are particularly well suited for selective and multiplexed monitoring, as monoamine NTs often coexist in biological systems; they need to be detected either simultaneously or individually without cross-interference. Commonly used CNSs include GO, RGO, CNTs (single-, multi-walled, and functionalized), and carbon black. More specialized CNSs, such as magnetically reduced GO, pyrolytic graphite, LIG, oxidized or acid-treated carbons, and conductive carbon textiles (fibers, clothes, and yarns) have also been employed. In contrast, sensors targeting non-monoamine NTs such as glutamate, acetylcholine, adenosine, and neuropeptide Y typically require catalytic substrates or biorecognition elements, as these analytes are not easily oxidizable. To address this, researchers have incorporated metal nanomaterials (noble and transition metal nanoparticles, MOFs, MXenes), metal oxides (ZnO, CuO, MnO_2, SnO_2, and layered oxides), conducting polymers (PANI, PEI, PEDOT:PSS, PPY), and Prussian blue analogues. For highly challenging targets, biocatalysts, including enzymes, antibodies, and aptamers, have been employed to achieve selective binding and quantification.

Across both monoamine and non-monoamine NTs, conducting substrates such as CNSs and metal nanoparticles are frequently used to improve active surface area, catalytic activity, and conductivity. Functionalization techniques such as acid treatment, pre-oxidation, and dopant incorporation further enhance sensitivity and synergistic performance. Selectivity, a critical factor in NT detection due to the coexistence of structurally and electrochemically similar analytes, has been achieved through polymeric coatings and bio-derived layers. Examples include Nafion, PPD, enzymes, aptamers, and molecularly imprinted polymers (e.g., polypyrrole, polystyrene), which enable effective trapping and recognition of target NTs even in complex biological matrices. In summary, it is evident that among various NTs, monoamine-based neurotransmitters are more extensively explored compared to others, particularly in the context of flexible, wearable, and implantable sensors. This predominance may be attributed to the relative ease of developing sensing materials for monoamine NTs owing to their electroactive nature. However, despite this advantage, achieving high selectivity for monoamines and other NTs in real-life scenarios remains a significant challenge, as they often coexist with structurally and electrochemically similar analytes. Therefore, more focused research is needed to address these limitations, with particular emphasis on the

Table 4
Analytical performances of other NT sensors.

Sensors	Substrates	Types	Analyte	Linear range (μM)	LOD (nM)	Sensitivity	Techniques	Real samples	Ref.
ACh/CB-PVC	Cotton yarn	Flexible	ACh	1–1 × 10^3	2.6 × 10^2	56.11 mV/dec	Potentiometric	Sheep brain	[104]
α-MnO_2/Cu-MOF-RGO	Carbon cloth	Flexible	ACh	0.1–3 × 10^3	5	–	AMP	Live cells, serum and urine	[105]
CuCo-MWCNT	Polyimide	Flexible	ACh	0.01–0.5	0.8	–	CV	Live cells	[106]
ACh-cocktail/LIG	Polyimide	Flexible	ACh	100–1 × 10^4	3.6 × 10^4	1.8 mV/dec	Potentiometric	Artificial CSF, brain tissue	[107]
MB/Apt-GNC-RGO/Pt	Pt rod	Implantable	ADO	1 × 10^{-4} – 1 × 10^3	0.1	–	DPV	Rat model	[108]
PoPD/Multienzyme/ PEI@GO/PB	Pt rod	Implantable	ADO	0–50	130	1.1 nA μM^{-1}	AMP	Rat model	[109]
Ab-thiol-AuE	Polyimide	Flexible/ Portable	NPY	10–500*	10*	–	AMP	Human sweat	[111]
Ab-EG3/PEDOT/ PPY	OHP sheet	Flexible	NPY	1–1 × 10^6*	0.68*	–	CA	Artificial sweat	[112]

Ab – Antibody; Apt – Aptamer; AuE – Gold electrode; CB – Carbon black; CSF – Cerebrospinal fluid; EG3 – Triethylene glycol; GNC – Gold nanocrystal; GO – Graphene oxide; LIG – Laser induced graphene; MB – Methylene blue; OHP – Overhead projector; PB – Prussian blue; PEI – Polyethyleneimine; PoPD – Poly-*o*-phenylenediamine; PPY – Polypyrrole; PVC – Polyvinyl alcohol; RGO – Reduced graphene oxide; Multienzyme - Adenosine deaminase, nucleoside phosphorylase, and xanthine oxidase; *pg mL^{-1}.

mechanistic aspects of NT sensing. Such insights could pave the way for the design of custom-made materials and task-specific recognition elements that interact selectively with target NTs, thereby enabling reliable, real-time monitoring in complex biological environments.

4. Significance of wearable and implantable sensors

In general, for wearable and implantable sensors to be truly practical, they must demonstrate high sensitivity and selectivity, biocompatibility, low detection limits, and long-term operational stability. Wearable sensors (WS) are typically placed on or just beneath the skin surface and most often measure target analytes from sweat, tears, or interstitial fluid (in the case of microneedle-based systems). Their performance is however, influenced by motion artifacts, ambient temperature, humidity, mechanical strain, variations in sweat secretion and evaporation, and potential interference from external contaminants such as dust and pollution, making stable and consistent analyte quantification challenging [113,114]. While WS are easy to use, modify, and replace, their accuracy can be compromised by these external factors. Nevertheless, they are excellent candidates for short-term monitoring as they are largely non-invasive, user-friendly, cost-effective, versatile, and require no expert assistance for application or removal [115]. Compared with PoCs, WS offer clear advantages in terms of continuous and autonomous monitoring, and they can be used in both passive conditions (e.g., rest or leisure) and active states (e.g., exercise, sports). A major drawback, however, is the poor or sometimes unknown correlation between biomarker concentrations in sweat and their actual systemic levels, which reduces their reliability relative to implantable systems [116]. Beyond these intrinsic challenges, WS faces additional barriers before large-scale clinical translation. One critical issue is the lack of robust calibration and standardization protocols. Variability in sweat composition between individuals, and even within the same individual under different physiological and environmental conditions, can compromise reproducibility and reliability. Dynamic calibration strategies or the integration of internal standards are being explored to mitigate these limitations [117,118]. Another important constraint is the requirement for a continuous power supply. Most WS rely on batteries, which limit long-term operation and increase device bulk. Recent advances in energy harvesting, such as motion-driven generators [119], sweat-based biofuel cells [120], and lightweight, flexible solar modules [121], offer promising alternatives for self-powered devices [122]. Furthermore, as WS are often connected to smartphones or cloud platforms, data security and patient privacy have become essential considerations for their clinical adoption [123]. On the positive side, WS are advancing toward multiplexed platforms capable of simultaneously detecting electrolytes, metabolites, and hormones, integrated with flexible electronics and wireless data transmission, thereby pushing the field toward comprehensive and more personalized health monitoring.

Implantable sensors (IMS), on the other hand, provide higher accuracy and reliability than WS. Positioned directly inside the body, they have real-time access to target biomarkers by interfacing with blood, cerebrospinal fluid, or interstitial fluid, thereby generating more stable and physiologically relevant analyte concentrations. However, this advantage comes with added complexity, as both implantation and removal require clinical expertise. IMS are also susceptible to biofouling, tissue encapsulation, and immune responses such as oxidative stress, inflammation, and disruption of the blood-brain barrier. Careful evaluation of the toxicity profile of the implant and sensing materials is therefore essential. To address these challenges, recent studies have explored various strategies to suppress or mitigate foreign-body responses. For example, coating implants with antioxidative enzymes can neutralize reactive oxygen species generated during implantation, thereby promoting inflammation-free integration [65]. Similarly, soft and flexible probes that mimic the mechanical properties of surrounding tissues enable the implant to move naturally with tissue motion, reducing micromotion-induced tears and subsequent inflammatory responses [89]. Developing ultra-small implants further minimizes tissue mismatch, lowering the risk of inflammation and related complications. Localized therapeutic hypothermia has also been shown to significantly suppress cytokine expression following implantation [124]. Biofouling remains another critical concern, as protein adsorption and biomolecule deposition gradually lead to electrode passivation and diminished performance, particularly during chronic use. To overcome this, surface modifications that alter polarity or hydrophobic/hydrophilic balance have been investigated to repel oppositely charged species, thereby reducing biofouling and passivation. Beyond material and biological considerations, IMS faces additional engineering challenges, particularly with respect to wireless communication and power transfer. These features are essential for practical use, as tethered implants are unsuitable for long-term monitoring. Current research is therefore focused on wireless power transfer strategies, including NFC-powered [125], radiofrequency communication [126], and ultrasound-based power delivery [127] to achieve miniaturized, battery-free, and maintenance-free operation [128]. Researchers are also focusing on developing IMS with self-destruction capabilities, which allow the devices to disintegrate autonomously or on demand after a defined period of operation. This approach eliminates the need for secondary surgery to remove the IMS, making such implants more user-friendly and less invasive [129]. Finally, IMS must overcome stringent regulatory and ethical hurdles before clinical translation. As invasive medical devices, they require extensive biocompatibility testing, comprehensive toxicity evaluation, long-term safety validation, and compliance with regulatory frameworks, alongside ethical considerations related to surgical implantation and chronic patient monitoring. Despite these obstacles, IMS offers distinct advantages for real-time, continuous monitoring and integration with closed-loop therapeutic systems, such as adaptive neurostimulation or on-demand drug delivery, positioning them as a transformative technology for chronic disease management and personalized medicine.

5. Summary and prospects

Neurotransmitters are chemical messengers that play a crucial role in maintaining normal physiological functions. As integral components of the CNS, they regulate essential processes such as heartbeat, memory, learning, digestion, and sleep. Imbalances in NT levels are strongly associated with a wide range of neurodegenerative and psychiatric disorders. Therefore, accurate quantification of NTs in bodily fluids provides valuable insights into both physical and mental health. Due to their ultralow concentrations and structural similarities, the selective and highly sensitive detection of individual NTs remains a significant analytical challenge. A variety of analytical techniques have been employed for NT detection, including chromatography, spectroscopy, colorimetry, fluorometry, and microdialysis. Nevertheless, these approaches are often expensive, time-consuming, complex, and reliant on sophisticated instrumentation and skilled personnel. Conventional diagnostics, typically involving blood, urine, or serum analysis, are often restricted to clinical settings and can be invasive, requiring repeated sample collection procedures that may be uncomfortable or distressing for patients. In contrast to conventional methods, advancements in wearable electronics have enabled non-invasive, real-time health monitoring, providing efficient alternatives to traditional diagnostic procedures. These technologies facilitate a shift from bulky laboratory instruments to compact, chip-based platforms capable of continuous health tracking in home-based or remote settings. Electrochemical methods have gained significant attention due to their rapid response, high sensitivity and selectivity, cost-effectiveness, ease of operation, and potential for miniaturization. With their high temporal and spatial resolution, electrochemical sensors are particularly well suited for NT analysis [130–132].

Despite the development of hundreds of electrochemical NT sensors, most rely on rigid electrodes, with only a few adapted for flexible or

wearable formats. This highlights a major disconnect between laboratory-based research and real-time, practical applications. Most of the existing work remains at the "proof-of-concept" stage—demonstrating potential performance but lacking critical steps toward real-time application and commercialization. For instance, many studies do not extend beyond laboratory testing, with only a small number exploring in vivo models or animal studies. Moreover, essential aspects such as validation in real biological samples, operation under realistic physiological conditions, and benchmarking against standard analytical methods are often missing, limiting the reliability of reported on-body results. Additionally, several fundamental challenges remain in the electrochemical sensing of NTs. Electrochemical sensors are inherently restricted to detecting electroactive analytes; for non-electroactive NTs, molecular imprinting, or indirect detection strategies such as labeling or the use of redox probes are required [133]. While many sensors perform well under controlled laboratory conditions, real biological samples present a far greater challenge. NTs are often found at ultralow concentrations in biofluids, necessitating extremely sensitive detection systems. Sensitivity can be enhanced by doping or decorating electrode materials with heteroatoms or noble metal nanoparticles. However, when employing such modifications, careful consideration of the biosafety and potential toxicity of these materials is essential. Furthermore, in biological environments, NTs coexist with interfering substances at concentrations 100 to 1000 times higher. This demands sensors with exceptional selectivity to ensure accurate quantification without interference. Selectivity can be improved by incorporating permselective membranes (e.g., Nafion, PPD), polymer imprinting, or electrostatically polarizing the sensor surface to repel similarly charged interferents. Nevertheless, introducing selectivity layers must be approached with caution, as they can unintentionally reduce the sensor's overall sensitivity. Therefore, future research should focus on the rational design and fabrication of electrocatalysts that are not only highly sensitive but also exhibit outstanding specificity under real-sample conditions.

From a fabrication standpoint, current flexible, wearable, and implantable NT sensors often use plastic films or thin substrates due to their flexibility, lightweight nature, and compatibility with body surfaces. However, the fabrication of such sensors typically involves methods like laser patterning, CVD, atomic layer deposition, sputtering, lithography techniques, spray coating, and more. These techniques often require complex, costly equipment, specialized training, and skilled personnel. Therefore, scalable and easy fabrication of the electrode platforms from readily available, inexpensive, and flexible materials are critical for advancing wearable and implantable biosensors. Another major challenge lies in the integration of sensors with flexible electronics capable of real-time data acquisition, processing, and wireless transmission to portable devices or cloud platforms. Without such integration, the practical utility of NT sensors for continuous monitoring and clinical use remains restricted. Addressing these challenges requires more systematic exploration of materials, architectures, and fabrication strategies tailored explicitly for wearable and implantable applications.

Looking ahead, the ultimate goal of developing wearable and implantable electrochemical sensing system is to create advanced closed-loop platforms capable of dynamically monitoring NT levels in the biological system and initiating real-time therapeutic interventions, such as targeted drug release or adaptive neural stimulation (Fig. 14). Achieving this vision requires the development of ultra-sensitive, highly specific, and biocompatible sensing interfaces that can operate reliably in vivo over extended periods. Future efforts should focus on engineering novel electrocatalytic materials, robust flexible substrates, and fully integrated systems that combine sensing, processing, and wireless communication. In conclusion, electrochemical sensors possess unique capabilities that make them ideal candidates for real-time, in vivo NT quantification. While their clinical and diagnostic applications remain underexplored, continued innovation in materials, fabrication, and integration strategies will pave the way for next-generation healthcare technologies. We believe this review will inspire further research in this promising field, driving progress toward overcoming current analytical challenges and enabling personalized, real-time neurochemical monitoring.

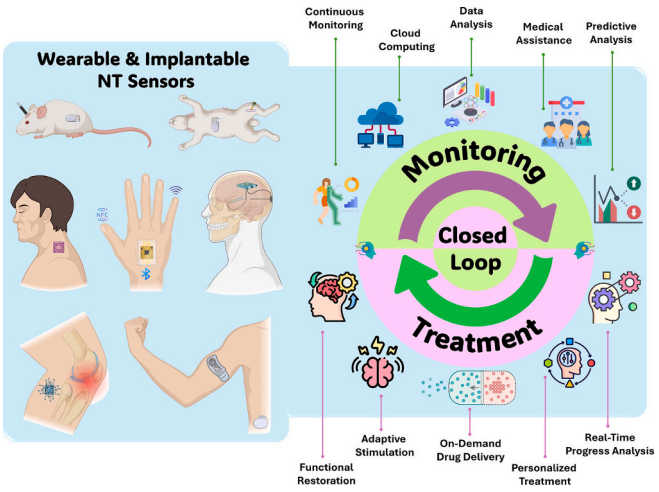

Fig. 14. Graphical illustration of futuristic applications of wearable and implantable NT sensors for closed-loop monitoring systems. The various shapes used in this figure were adapted from biorender.com and flaticon.com.

CRediT statement

K.T. – Conceptualization; Methodology; Writing original draft, reviewing and editing; Visualization. L.Z. – Methodology; Writing original draft and editing. Y-J.K. – Conceptualization; Methodology; Writing - reviewing and editing; Supervision; Funding acquisition. All the authors have read and agreed to the final version of the manuscript.

Declaration of competing interest

The authors declare that they have no known competing financial interests or personal relationships that could have appeared to influence the work reported in this paper.

Acknowledgements

This work was funded by the National Research Foundation of Korea (Grant number: NRF-2022R1F1A1074346, RS-2024-00433166).

Data availability

No data was used for the research described in the article.

References

[1] Y. Mei, Q.-W. Zhang, Q. Gu, Z. Liu, X. He, Y. Tian, Pillar[5]arene-based fluorescent sensor array for biosensing of intracellular multi-neurotransmitters through host–guest recognitions, J. Am. Chem. Soc. 144 (2022) 2351–2359, https://doi.org/10.1021/jacs.1c12959.
[2] J. He, E. Spanolios, C.E. Froehlich, C.L. Wouters, C.L. Haynes, Recent advances in the development and characterization of electrochemical and electrical biosensors for small molecule neurotransmitters, ACS Sens. 8 (2023) 1391–1403, https://doi.org/10.1021/acssensors.3c00082.
[3] R. Liu, Z.-Y. Feng, D. Li, B. Jin, Y. Lan, L.-Y. Meng, Recent trends in carbon-based microelectrodes as electrochemical sensors for neurotransmitter detection: a review, TrAC, Trends Anal. Chem. 148 (2022) 116541, https://doi.org/10.1016/j.trac.2022.116541.
[4] Y. Qi, D. Jang, J. Ryu, T. Bai, Y. Shin, W. Gu, A. Iyer, G. Li, H. Ma, J. Liou, M. Van Der Meer, Y. Qiang, H. Fang, Stabilized carbon coating on microelectrodes for scalable and interoperable neurotransmitter sensing, Nat. Commun. 16 (2025) 3300, https://doi.org/10.1038/s41467-025-58388-z.
[5] E.M. Tansey, Henry dale and the discovery of acetylcholine, C. R. Biol. 329 (2006) 419–425, https://doi.org/10.1016/j.crvi.2006.03.012.

[6] Y. Yang, L. Sun, X. Liu, W. Liu, Z. Zhang, X. Zhou, X. Zhao, R. Zheng, Y. Zhang, W. Guo, X. Wang, X. Li, J. Pang, F. Li, Y. Tao, D. Shi, W. Shen, L. Wang, J. Zang, S. Li, Neurotransmitters: impressive regulators of tumor progression, Biomed. Pharmacother. 176 (2024) 116844, https://doi.org/10.1016/j.biopha.2024.116844.
[7] M. Hasanzadeh, N. Shadjou, M.D.L. Guardia, Current advancement in electrochemical analysis of neurotransmitters in biological fluids, TrAC, Trends Anal. Chem. 86 (2017) 107–121, https://doi.org/10.1016/j.trac.2016.11.001.
[8] S.B. Park, B. Koh, H.S. Kwon, Y.E. Kim, S.S. Kim, S.-H. Cho, T.-Y. Kim, M.A. Bae, D. Kang, C.H. Kim, K.Y. Kim, Quantitative and qualitative analysis of neurotransmitter and neurosteroid production in cerebral organoids during differentiation, ACS Chem. Neurosci. 14 (2023) 3761–3771, https://doi.org/10.1021/acschemneuro.3c00246.
[9] M.D. Condon, N.J. Platt, Y.-F. Zhang, B.M. Roberts, M.A. Clements, S. Vietti-Michelina, M.-Y. Tseu, K.R. Brimblecombe, S. Threlfell, E.O. Mann, S.J. Cragg, Plasticity in striatal dopamine release is governed by release-independent depression and the dopamine transporter, Nat. Commun. 10 (2019) 4263, https://doi.org/10.1038/s41467-019-12264-9.
[10] Y. Da, S. Luo, Y. Tian, Real-time monitoring of neurotransmitters in the brain of living animals, ACS Appl. Mater. Interfaces 15 (2023) 138–157, https://doi.org/10.1021/acsami.2c02740.
[11] M. Oshaghi, M. Kourosh-Arami, M. Roozbehkia, Role of neurotransmitters in immune-mediated inflammatory disorders: a crosstalk between the nervous and immune systems, Neurol. Sci. 44 (2023) 99–113, https://doi.org/10.1007/s10072-022-06413-0.
[12] L.-L. Gao, E.-Q. Gao, Metal–organic frameworks for electrochemical sensors of neurotransmitters, Coord. Chem. Rev. 434 (2021) 213784, https://doi.org/10.1016/j.ccr.2021.213784.
[13] R.R. Poolakkandy, M.M. Menamparambath, Transition metal oxide based non-enzymatic electrochemical sensors: an arising approach for the meticulous detection of neurotransmitter biomarkers, Electrochem. Sci. Adv. 1 (2021) e2000024, https://doi.org/10.1002/elsa.202000024.
[14] G. Burns, M.Y. Ali, M.M.R. Howlader, Advanced functional materials for electrochemical dopamine sensors, TrAC, Trends Anal. Chem. 169 (2023) 117367, https://doi.org/10.1016/j.trac.2023.117367.
[15] F. Oukhatar, S. Même, W. Même, F. Szeremeta, N.K. Logothetis, G. Angelovski, É. Tóth, MRI sensing of neurotransmitters with a crown ether appended Gd^{3+} complex, ACS Chem. Neurosci. 6 (2015) 219–225, https://doi.org/10.1021/cn500289y.
[16] H. Kaur, S.S. Siwal, R.V. Saini, N. Singh, V.K. Thakur, Significance of an electrochemical sensor and nanocomposites: toward the electrocatalytic detection of neurotransmitters and their importance within the physiological system, ACS Nanosci. Au 3 (2023) 1–27, https://doi.org/10.1021/acsnanoscienceau.2c00039.
[17] S. Madhurantakam, J.B. Karnam, D. Brabazon, M. Takai, I.U. Ahad, J.B. Balaguru Rayappan, U.M. Krishnan, "Nano": an emerging avenue in electrochemical detection of neurotransmitters, ACS Chem. Neurosci. 11 (2020) 4024–4047, https://doi.org/10.1021/acschemneuro.0c00355.
[18] D. Mohanapriya, J. Satija, S. Senthilkumar, V. Kumar Ponnusamy, K. Thenmozhi, Design and engineering of 2D MXenes for point-of-care electrochemical detection of bioactive analytes and environmental pollutants, Coord. Chem. Rev. 507 (2024) 215746, https://doi.org/10.1016/j.ccr.2024.215746.
[19] K. Theyagarajan, V.P. Sruthi, J. Satija, S. Senthilkumar, Y.-J. Kim, Materials and design strategies for the electrochemical detection of antineoplastic drugs: Progress and perspectives, Mater. Sci. Eng. R 161 (2024) 100840, https://doi.org/10.1016/j.mser.2024.100840.
[20] S.G. Chavan, P.R. Rathod, A. Koyappayil, S. Hwang, M.-H. Lee, Recent advances of electrochemical and optical point-of-care biosensors for detecting neurotransmitter serotonin biomarkers, Biosens. Bioelectron. 267 (2025) 116743, https://doi.org/10.1016/j.bios.2024.116743.
[21] M. Chandran, M. Veerapandian, B. Dhanasekaran, S. Govindaraju, K. Yun, Advanced nanomaterials for health monitoring and diagnostics in next-generation wearable sensors, Mater. Sci. Eng. R 165 (2025) 101015, https://doi.org/10.1016/j.mser.2025.101015.
[22] K. Theyagarajan, Y.-J. Kim, Metal organic frameworks based wearable and point-of-care electrochemical sensors for healthcare monitoring, Biosensors 14 (2024) 492, https://doi.org/10.3390/bios14100492.
[23] J.B. Holman, A.E. Oseyemi, M. Koumbia, Z. Shi, C. Li, W. Ding, The rise of eco-friendly electronics: exploring wearable paper-based electroanalytical devices, Mater. Sci. Eng. R 163 (2025) 100939, https://doi.org/10.1016/j.mser.2025.100939.
[24] K.V. Ratnam, H. Manjunatha, S. Janardan, K.C. Babu Naidu, S. Ramesh, Nonenzymatic electrochemical sensor based on metal oxide, MO (M= cu, Ni, Zn, and Fe) nanomaterials for neurotransmitters: an abridged review, Sens. Int. 1 (2020) 100047, https://doi.org/10.1016/j.sintl.2020.100047.
[25] J.-M. Moon, N. Thapliyal, K.K. Hussain, R.N. Goyal, Y.-B. Shim, Conducting polymer-based electrochemical biosensors for neurotransmitters: a review, Biosens. Bioelectron. 102 (2018) 540–552, https://doi.org/10.1016/j.bios.2017.11.069.
[26] K. Theyagarajan, Y.-J. Kim, Recent developments in the design and fabrication of electrochemical biosensors using functional materials and molecules, Biosensors 13 (2023) 424, https://doi.org/10.3390/bios13040424.
[27] E. Kipkorir, O. Kimani, Electrochemical sensing of pharmaceutical pollutants using modified glassy carbon electrodes with nanostructures: a review, Inorg. Chem. Commun. 179 (2025) 114827, https://doi.org/10.1016/j.inoche.2025.114827.
[28] A. Azzouz, K.Y. Goud, N. Raza, E. Ballesteros, S.-E. Lee, J. Hong, A. Deep, K.-H. Kim, Nanomaterial-based electrochemical sensors for the detection of neurochemicals in biological matrices, TrAC, Trends Anal. Chem. 110 (2019) 15–34, https://doi.org/10.1016/j.trac.2018.08.002.
[29] R.S. Perala, N. Chandrasekar, R. Balaji, P.S. Alexander, N.Z.N. Humaidi, M. T. Hwang, A comprehensive review on graphene-based materials: from synthesis to contemporary sensor applications, Mater. Sci. Eng. R 159 (2024) 100805, https://doi.org/10.1016/j.mser.2024.100805.
[30] K. Theyagarajan, B.A. Lakshmi, C. Kim, Y.-J. Kim, A nanohybrid-based smartphone-compatible high performance electrochemical glucose sensor, Mater. Today Chem. 41 (2024) 102282, https://doi.org/10.1016/j.mtchem.2024.102282.
[31] P. Wei, W. Han, L. Xie, L. Zhu, B. He, X. Cao, Research progress on nanomaterial-based electrochemical sensors for the detection of aflatoxin B1 in food and environmental samples, Chem. Eng. J. 509 (2025) 160902, https://doi.org/10.1016/j.cej.2025.160902.
[32] A. Cetinkaya, S.I. Kaya, M. Yence, F. Budak, S.A. Ozkan, Ionic liquid-based materials for electrochemical sensor applications in environmental samples, Trends Environ. Anal. Chem. 37 (2023) e00188, https://doi.org/10.1016/j.teac.2022.e00188.
[33] M. Sajid, N. Baig, K. Alhooshani, Chemically modified electrodes for electrochemical detection of dopamine: challenges and opportunities, TrAC, Trends Anal. Chem. 118 (2019) 368–385, https://doi.org/10.1016/j.trac.2019.05.042.
[34] Z. Shao, Y. Chang, B.J. Venton, Carbon microelectrodes with customized shapes for neurotransmitter detection: a review, Anal. Chim. Acta 1223 (2022) 340165, https://doi.org/10.1016/j.aca.2022.340165.
[35] Y. Yang, W. Gao, Wearable and flexible electronics for continuous molecular monitoring, Chem. Soc. Rev. 48 (2019) 1465–1491, https://doi.org/10.1039/C7CS00730B.
[36] X. Li, Z.-Y. Zhang, F. Li, Flexible electrochemical sensors based on nanomaterials: constructions, applications and prospects, Chem. Eng. J. 504 (2025) 158101, https://doi.org/10.1016/j.cej.2024.158101.
[37] F. Gao, C. Liu, L. Zhang, T. Liu, Z. Wang, Z. Song, H. Cai, Z. Fang, J. Chen, J. Wang, M. Han, J. Wang, K. Lin, R. Wang, M. Li, Q. Mei, X. Ma, S. Liang, G. Gou, N. Xue, Wearable and flexible electrochemical sensors for sweat analysis: a review, Microsyst. Nanoeng. 9 (2023) 1, https://doi.org/10.1038/s41378-022-00443-6.
[38] K.A. Alamry, M.A. Hussein, J. Choi, W.A. El-Said, Non-enzymatic electrochemical sensor to detect γ-aminobutyric acid with ligand-based on graphene oxide modified gold electrode, J. Electroanal. Chem. 879 (2020) 114789, https://doi.org/10.1016/j.jelechem.2020.114789.
[39] Y. Li, H. Wei, Y. Chen, J. Ma, X. Zhang-Peng, W. Li, F. Hu, A novel flexible electrochemical molecular imprinted sensor for the determination of GABA in serum of depressed mice, J. Electrochem. Soc. 170 (2023) 017504, https://doi.org/10.1149/1945-7111/acb236.
[40] S.S. Chu, H.A. Nguyen, D. Lin, M. Bhatti, C.E. Jones-Tinsley, A.H. Do, R. D. Frostig, Z. Nenadic, X. Xu, M.M. Lim, H. Cao, Development of highly sensitive, flexible dual L-glutamate and GABA microsensors for in vivo brain sensing, Biosens. Bioelectron. 222 (2023) 114941, https://doi.org/10.1016/j.bios.2022.114941.
[41] M.S. Hernandes, L.R.P. Troncone, Glycine as a neurotransmitter in the forebrain: a short review, J. Neural Transm. 116 (2009) 1551–1560, https://doi.org/10.1007/s00702-009-0326-6.
[42] W. Ling, G. Liew, Y. Li, Y. Hao, H. Pan, H. Wang, B. Ning, H. Xu, X. Huang, Materials and techniques for implantable nutrient sensing using flexible sensors integrated with metal–organic frameworks, Adv. Mater. 30 (2018) 1800917, https://doi.org/10.1002/adma.201800917.
[43] E.M. Robbins, B. Wong, M.Y. Pwint, S. Salavatian, A. Mahajan, X.T. Cui, Improving sensitivity and longevity of in vivo glutamate sensors with electrodeposited nanoPt, ACS Appl. Mater. Interfaces 16 (2024) 40570–40580, https://doi.org/10.1021/acsami.4c06692.
[44] R.R. Poolakkandy, N. Ar, K.A. Padmalayam, R.G.K.M.M. Menamparambath, Nickel hydroxide nanoflake/carbon nanotube composites for the electrochemical detection of glutamic acid using in vitro stroke model, ACS Appl. Nano Mater. 6 (2023) 1347–1359, https://doi.org/10.1021/acsanm.2c04989.
[45] A. Weltin, J. Kieninger, B. Enderle, A.-K. Gellner, B. Fritsch, G.A. Urban, Polymer-based, flexible glutamate and lactate microsensors for in vivo applications, Biosens. Bioelectron. 61 (2014) 192–199, https://doi.org/10.1016/j.bios.2014.05.014.
[46] T.N.H. Nguyen, J.K. Nolan, H. Park, S. Lam, M. Fattah, J.C. Page, H.-E. Joe, M.B. G. Jun, H. Lee, S.J. Kim, R. Shi, H. Lee, Facile fabrication of flexible glutamate biosensor using direct writing of platinum nanoparticle-based nanocomposite ink, Biosens. Bioelectron. 131 (2019) 257–266, https://doi.org/10.1016/j.bios.2019.01.051.
[47] X. Wen, B. Wang, S. Huang, T. Leo Liu, M.-S. Lee, P.-S. Chung, Y.T. Chow, I.-W. Huang, H.G. Monbouquette, N.T. Maidment, P.-Y. Chiou, Flexible, multifunctional neural probe with liquid metal enabled, ultra-large tunable stiffness for deep-brain chemical sensing and agent delivery, Biosens. Bioelectron. 131 (2019) 37–45, https://doi.org/10.1016/j.bios.2019.01.060.
[48] C. Liu, X. Lin, J. Liao, M. Yang, M. Jiang, Y. Huang, Z. Du, L. Chen, S. Fan, Q. Huang, Carbon dots-based dopamine sensors: recent advances and challenges, Chin. Chem. Lett. 35 (2024) 109598, https://doi.org/10.1016/j.cclet.2024.109598.
[49] A. Karim, M. Yasser, A. Ahmad, H. Natsir, A. Wahid Wahab, P. Taba St. Fauziah, I. Pratama, A. Rajab Rosalin, A. Nur Fitriani Abubakar, T. Widayati Putri,

R. Munadi, A. Fudhail Majid, A. Nur, A. Rifai Fadliah, M. Syahrir, A review: Progress and trend advantage of dopamine electrochemical sensor, J. Electroanal. Chem. 959 (2024) 118157, https://doi.org/10.1016/j.jelechem.2024.118157.
[50] K. Nishimura, T. Ushiyama, N.X. Viet, M. Inaba, S. Kishimoto, Y. Ohno, Enhancement of the electron transfer rate in carbon nanotube flexible electrochemical sensors by surface functionalization, Electrochim. Acta 295 (2019) 157–163, https://doi.org/10.1016/j.electacta.2018.10.147.
[51] N.X. Viet, S. Kishimoto, Y. Ohno, Highly uniform, flexible microelectrodes based on the clean single-walled carbon nanotube thin film with high electrochemical activity, ACS Appl. Mater. Interfaces 11 (2019) 6389–6395, https://doi.org/10.1021/acsami.8b19252.
[52] Y. Zhou, Y. Cai, T. Tu, S. Zhang, T. Li, L. Fang, D. Wang, Y. Liang, Z. Wang, Y. Jiang, C. Zhou, B. Liang, Expanded carbon nanotube fiber at the liquid–air interface for high-performance fiber-based supercapacitors and electrochemical sensors, ACS Appl. Mater. Interfaces 15 (2023) 41839–41849, https://doi.org/10.1021/acsami.3c06815.
[53] D. Ghosh, R. Tabassum, P.P. Sarkar, M.A. Rahman, A.H. Jalal, N. Islam, A. Ashraf, Graphene nanocomposite ink coated laser transformed flexible electrodes for selective dopamine detection and immunosensing, ACS Appl. Bio Mater. 7 (2024) 3143–3153, https://doi.org/10.1021/acsabm.4c00166.
[54] Z. Shi, X. Wu, Z. Zou, L. Yu, F. Hu, Y. Li, C. Guo, C.M. Li, Screen-printed analytical strip constructed with bacteria-templated porous N-doped carbon nanorods/au nanoparticles for sensitive electrochemical detection of dopamine molecules, Biosens. Bioelectron. 186 (2021) 113303, https://doi.org/10.1016/j.bios.2021.113303.
[55] K.M.R.L.R. Panicker, R. Narayan, Y.G. Kotagiri, Biopolymer-protected graphene-Fe_3O_4 nanocomposite based wearable microneedle sensor: toward real-time continuous monitoring of dopamine, RSC Adv. 14 (2024) 7131–7141, https://doi.org/10.1039/D4RA00110A.
[56] V. Rajendiran, D.H. Kim, A. Krishnakumar, P. Dhivya, K. Tsuchiya, Y. Sunami, G. K. Mani, Cleanroom-free fabrication of flexible microneedle array patches for minimally invasive monitoring of dopamine, J. Electron. Mater. 53 (2024) 6243–6249, https://doi.org/10.1007/s11664-024-11338-9.
[57] X. Qing, J. Wu, Q. Shu, D. Wang, M. Li, D. Liu, X. Wang, W. Lei, High gain fiber-shaped transistor based on rGO-mediated hierarchical polypyrrole for ultrasensitive sweat sensor, Sens. Actuators, A 354 (2023) 114297, https://doi.org/10.1016/j.sna.2023.114297.
[58] S. Uruc, E. Dokur, R. Kurteli, O. Gorduk, Y. Sahin, Heteroatom-doped graphene oxide-based conductive ink: synthesis, characterization and investigation of the conductivity properties for flexible sensor technology, New J. Chem. 47 (2023) 12360–12374, https://doi.org/10.1039/D3NJ01525D.
[59] S. Farajikhah, P.C. Innis, B. Paull, G.G. Wallace, A.R. Harris, Facile development of a fiber-based electrode for highly selective and sensitive detection of dopamine, ACS Sens. 4 (2019) 2599–2604, https://doi.org/10.1021/acssensors.9b01583.
[60] C. Wang, Y. Zhang, Y. Liu, X. Zeng, C. Jin, D. Huo, J. Hou, C. Hou, A wearable flexible electrochemical biosensor with CuNi-MOF@rGO modification for simultaneous detection of uric acid and dopamine in sweat, Anal. Chim. Acta 1299 (2024) 342441, https://doi.org/10.1016/j.aca.2024.342441.
[61] Z. Song, R. Li, Z. Li, X. Luo, Antifouling and antimicrobial wearable electrochemical sweat sensors for accurate dopamine monitoring based on amyloid albumin composite hydrogels, Biosens. Bioelectron. 264 (2024) 116640, https://doi.org/10.1016/j.bios.2024.116640.
[62] Y. Wang, P. Zhao, B. Gao, M. Yuan, J. Yu, Z. Wang, X. Chen, Self-reduction of bimetallic nanoparticles on flexible MXene-graphene electrodes for simultaneous detection of ascorbic acid, dopamine, and uric acid, Microchem. J. 185 (2023) 108177, https://doi.org/10.1016/j.microc.2022.108177.
[63] L. Wang, W. Ou, H. Liu, S. Wang, Z. Xia, X. Wang, K. Yu, Electronic structure optimization of titanium-based layered oxide to boost flexible sensing performance, Appl. Surf. Sci. 618 (2023) 156702, https://doi.org/10.1016/j.apsusc.2023.156702.
[64] J. Chen, F. Xia, X. Ding, D. Zhang, Highly sensitive and biocompatible microsensor for selective dynamic monitoring of dopamine in rat brain, ACS Sens. 9 (2024) 6207–6217, https://doi.org/10.1021/acssensors.4c02109.
[65] X. Gao, H. Wei, W. Ma, W. Wu, W. Ji, J. Mao, P. Yu, L. Mao, Inflammation-free electrochemical in vivo sensing of dopamine with atomic-level engineered antioxidative single-atom catalyst, Nat. Commun. 15 (2024) 7915, https://doi.org/10.1038/s41467-024-52279-5.
[66] B. Patella, A. Sortino, F. Mazzara, G. Aiello, G. Drago, C. Torino, A. Vilasi, A. O'Riordan, R. Inguanta, Electrochemical detection of dopamine with negligible interference from ascorbic and uric acid by means of reduced graphene oxide and metals-NPs based electrodes, Anal. Chim. Acta 1187 (2021) 339124, https://doi.org/10.1016/j.aca.2021.339124.
[67] Y. Ma, Z. Wei, Y. Wang, Y. Ding, L. Jiang, X. Fu, Y. Zhang, J. Sun, W. Zhu, J. Wang, Surface oxygen functionalization of carbon cloth toward enhanced electrochemical dopamine sensing, ACS Sustain. Chem. Eng. 9 (2021) 16063–16072, https://doi.org/10.1021/acssuschemeng.1c03430.
[68] M.K.P.O.I. Shown, L.-C. Chen, K.-H. Chen, Y. Tai, Flexible sensor for dopamine detection fabricated by the direct growth of α-Fe_2O_3 nanoparticles on carbon cloth, Appl. Surf. Sci. 427 (2018) 387–395, https://doi.org/10.1016/j.apsusc.2017.08.168.
[69] S. Madhu, P. Manickam, M. Pierre, S. Bhansali, P. Nagamony, V. Chinnuswamy, Nanostructured SnO_2 integrated conductive fabrics as binder-free electrode for neurotransmitter detection, Sens. Actuators, A 269 (2018) 401–411, https://doi.org/10.1016/j.sna.2017.11.046.
[70] L. Zhao, Z. Cai, Q. Yao, T. Zhao, H. Lin, Y. Xiao, X. Chen, Electropolymerization fabrication of three-dimensional N, P-co-doped carbon network as a flexible electrochemical dopamine sensor, Sensors Actuators B Chem. 253 (2017) 1113–1119, https://doi.org/10.1016/j.snb.2017.06.111.
[71] M. Şen, M. Oğuz, İ. Avcı, Non-toxic flexible screen-printed MWCNT-based electrodes for non-invasive biomedical applications, Talanta 268 (2024) 125341, https://doi.org/10.1016/j.talanta.2023.125341.
[72] H. Cheng, W. Jin, X. Huang, X. Liu, F. Wang, X. Guo, Y. Wu, Y. Ying, Y. Wen, H. Yang, A flexible carbon nanotube-modified poly(styrene-butadiene)-based dopamine sensor, Nanotechnology 31 (2020) 015505, https://doi.org/10.1088/1361-6528/ab4373.
[73] N. Dhanjai, S.M. Yu, Mugo, a flexible-imprinted capacitive sensor for rapid detection of adrenaline, Talanta 204 (2019) 602–606, https://doi.org/10.1016/j.talanta.2019.06.016.
[74] N.M. Yousif, R.M. Attia, M.R. Balboul, Adrenaline biosensors based on rGO/ag nanocomposites functionalized textiles using advanced electron beam irradiation technique, J. Organomet. Chem. 972 (2022) 122392, https://doi.org/10.1016/j.jorganchem.2022.122392.
[75] G. Ibáñez-Redín, D. Wilson, D. Gonçalves, O.N. Oliveira, Low-cost screen-printed electrodes based on electrochemically reduced graphene oxide-carbon black nanocomposites for dopamine, epinephrine and paracetamol detection, J. Colloid Interface Sci. 515 (2018) 101–108, https://doi.org/10.1016/j.jcis.2017.12.085.
[76] I.A. De Araujo Andreotti, L.O. Orzari, J.R. Camargo, R.C. Faria, L.H. Marcolino-Junior, M.F. Bergamini, A. Gatti, B.C. Janegitz, Disposable and flexible electrochemical sensor made by recyclable material and low cost conductive ink, J. Electroanal. Chem. 840 (2019) 109–116, https://doi.org/10.1016/j.jelechem.2019.03.059.
[77] Y. Sun, H. Li, C. Li, L. Wang, X. Xuan, M. Li, Preparation of a cu/CuO-vertical graphene microelectrode for the simultaneous determination of epinephrine and 2-aminoadenosine, Mater. Today Chem. 33 (2023) 101685, https://doi.org/10.1016/j.mtchem.2023.101685.
[78] S.M. Mugo, S.V. Robertson, W. Lu, A molecularly imprinted screen-printed carbon electrode for electrochemical epinephrine, lactate, and cortisol metabolites detection in human sweat, Anal. Chim. Acta 1278 (2023) 341714, https://doi.org/10.1016/j.aca.2023.341714.
[79] S.M. Mugo, S.V. Robertson, W. Lu, A molecularly imprinted electrochemical microneedle sensor for multiplexed metabolites detection in human sweat, Talanta 259 (2023) 124531, https://doi.org/10.1016/j.talanta.2023.124531.
[80] D. Ji, Z. Shi, Z. Liu, S.S. Low, J. Zhu, T. Zhang, Z. Chen, X. Yu, Y. Lu, D. Lu, Q. Liu, Smartphone-based square wave voltammetry system with screen-printed graphene electrodes for norepinephrine detection, Smart Mater. Med. 1 (2020) 1–9, https://doi.org/10.1016/j.smaim.2020.02.001.
[81] S. Boobphahom, T. Siripongpreda, D. Zhang, J. Qin, P. Rattanawaleedirojn, N. Rodthongkum, TiO_2/MXene-PVA/GO hydrogel-based electrochemical sensor for neurological disorder screening via urinary norepinephrine detection, Microchim. Acta 188 (2021) 387, https://doi.org/10.1007/s00604-021-04945-4.
[82] M. Su, H. Lan, L. Tian, M. Jiang, X. Cao, C. Zhu, C. Yu, Ti_3C_2Tx-reduced graphene oxide nanocomposite-based electrochemical sensor for serotonin in human biofluids, Sensors Actuators B Chem. 367 (2022) 132019, https://doi.org/10.1016/j.snb.2022.132019.
[83] T.D. Thanh, J. Balamurugan, H.V. Hien, N.H. Kim, J.H. Lee, A novel sensitive sensor for serotonin based on high-quality of AuAg nanoalloy encapsulated graphene electrocatalyst, Biosens. Bioelectron. 96 (2017) 186–193, https://doi.org/10.1016/j.bios.2017.05.014.
[84] B. Guntupalli, P. Liang, J.-H. Lee, Y. Yang, H. Yu, J. Canoura, J. He, W. Li, Y. Weizmann, Y. Xiao, Ambient filtration method to rapidly prepare highly conductive, paper-based porous gold films for electrochemical biosensing, ACS Appl. Mater. Interfaces 7 (2015) 27049–27058, https://doi.org/10.1021/acsami.5b09612.
[85] H. Kim, A. Koyappayil, H. Seok, K. Aydin, C. Kim, K. Park, N. Jeon, W.S. Kang, M. Lee, T. Kim, Concurrent and selective determination of dopamine and serotonin with flexible WS_2/graphene/polyimide electrode using cold plasma, Small 17 (2021) 2102757, https://doi.org/10.1002/smll.202102757.
[86] S.G. Chavan, A.K. Yagati, A. Koyappayil, A. Go, S. Yeon, T. Lee, M.-H. Lee, Conformationally flexible dimeric-serotonin-based sensitive and selective electrochemical biosensing strategy for serotonin recognition, Anal. Chem. 94 (2022) 17020–17030, https://doi.org/10.1021/acs.analchem.2c02747.
[87] S.H. Ko, S.W. Kim, S.H. Lee, Y.J. Lee, Electrodeposited reduced graphene oxide-PEDOT:PSS/Nafion hybrid interface for the simultaneous determination of dopamine and serotonin, Sci. Rep. 13 (2023) 20274, https://doi.org/10.1038/s41598-023-47693-6.
[88] L.R. Panicker, F. Shamsheera, R. Narayan, Y.G. Kotagiri, Wearable electrochemical microneedle sensors based on the graphene-silver-chitosan nanocomposite for real-time continuous monitoring of the depression biomarker serotonin, ACS Appl. Nano Mater. 6 (2023) 20601–20611, https://doi.org/10.1021/acsanm.3c02976.
[89] E. Castagnola, E.M. Robbins, D.D. Krahe, B. Wu, M.Y. Pwint, Q. Cao, X.T. Cui, Stable in-vivo electrochemical sensing of tonic serotonin levels using PEDOT/CNT-coated glassy carbon flexible microelectrode arrays, Biosens. Bioelectron. 230 (2023) 115242, https://doi.org/10.1016/j.bios.2023.115242.
[90] J. Han, T. Ho, J.M. Stine, S.N. Overton, J. Herberholz, R. Ghodssi, simultaneous dopamine and serotonin monitoring in freely moving crayfish using a wireless electrochemical sensing system, ACS Sens. 9 (2024) 2346–2355, https://doi.org/10.1021/acssensors.3c02304.

[91] A.L. Herrald, E.K. Ambrogi, K.A. Mirica, Electrochemical detection of gasotransmitters: status and roadmap, ACS Sens. 9 (2024) 1682–1705, https://doi.org/10.1021/acssensors.3c02529.
[92] Z. Liu, H. Forsyth, N. Khaper, A. Chen, Sensitive electrochemical detection of nitric oxide based on AuPt and reduced graphene oxide nanocomposites, Analyst 141 (2016) 4074–4083, https://doi.org/10.1039/C6AN00429F.
[93] H. Xu, C. Liao, Y. Liu, B.-C. Ye, B. Liu, Iron phthalocyanine decorated nitrogen-doped graphene biosensing platform for real-time detection of nitric oxide released from living cells, Anal. Chem. 90 (2018) 4438–4444, https://doi.org/10.1021/acs.analchem.7b04419.
[94] Y. Zhang, S.-Y. Lu, Z. Shi, Z.L. Zhao, Q. Liu, J.-C. Gao, T. Liang, Z. Zou, C.M. Li, A multi-component Cu_2O@$FePO_4$ core–cage structure to jointly promote fast electron transfer toward the highly sensitive *in situ* detection of nitric oxide, Nanoscale 11 (2019) 4471–4477, https://doi.org/10.1039/C8NR10198A.
[95] M. Zhou, Y. Jiang, G. Wang, W. Wu, W. Chen, P. Yu, Y. Lin, J. Mao, L. Mao, Single-atom Ni-N_4 provides a robust cellular NO sensor, Nat. Commun. 11 (2020) 3188, https://doi.org/10.1038/s41467-020-17018-6.
[96] R. Li, H. Qi, Y. Ma, Y. Deng, S. Liu, Y. Jie, J. Jing, J. He, X. Zhang, L. Wheatley, C. Huang, X. Sheng, M. Zhang, L. Yin, A flexible and physically transient electrochemical sensor for real-time wireless nitric oxide monitoring, Nat. Commun. 11 (2020) 3207, https://doi.org/10.1038/s41467-020-17008-8.
[97] J. Li, M. Su, M. Jiang, L. Tian, C. Zhu, X. Cao, Q. Jiang, X. Huo, C. Yu, Stretchable conductive film based on silver nanowires and carbon nanotubes for real-time inducing and monitoring of cell-released NO, Sensors Actuators B Chem. 366 (2022) 131983, https://doi.org/10.1016/j.snb.2022.131983.
[98] H. Gao, W. Peng, Y. Zhou, Z. Ding, M. Su, Z. Wu, C. Yu, Flexible and multi-functional three-dimensional scaffold based on enokitake-like au nanowires for real-time monitoring of endothelial mechanotransduction, Biosens. Bioelectron. 263 (2024) 116610, https://doi.org/10.1016/j.bios.2024.116610.
[99] D.C. Patra, S.P. Mondal, Paper-based electrochemical sensor integrated with gold nanoparticle-decorated carbon cloth as a working electrode for nitric oxide detection in artificial tears, ACS Appl. Bio Mater. 7 (2024) 5247–5257, https://doi.org/10.1021/acsabm.4c00425.
[100] J. Li, C. Zhu, W. Peng, X. Cao, H. Gao, M. Jiang, Z. Wu, C. Yu, Stretchable electrochemical sensor based on a gold nanowire and carbon nanotube network for real-time tracking cell-released H_2S, Anal. Chem. 95 (2023) 2406–2412, https://doi.org/10.1021/acs.analchem.2c04477.
[101] Y. Xu, W. Huang, Y. Zhang, H. Duan, F. Xiao, Electrochemical microfluidic multiplexed bioanalysis by a highly active bottlebrush-like nanocarbon microelectrode, Anal. Chem. 94 (2022) 4463–4473, https://doi.org/10.1021/acs.analchem.1c05544.
[102] Y. Xu, W. Huang, H. Duan, F. Xiao, Bimetal−organic framework-integrated electrochemical sensor for on-chip detection of H_2S and H_2O_2 in cancer tissues, Biosens. Bioelectron. 260 (2024) 116463, https://doi.org/10.1016/j.bios.2024.116463.
[103] S. Shakil, D. Yuan, M. Li, Review—electrochemical sensors for acetylcholine detection, J. Electrochem. Soc. 171 (2024) 067512, https://doi.org/10.1149/1945-7111/ad546e.
[104] F. Amirghasemi, A. Soleimani, S. Bawarith, A. Tabassum, A. Morrel, M.P. S. Mousavi, FAST (flexible acetylcholine sensing thread): real-time detection of acetylcholine with a flexible solid-contact potentiometric sensor, Bioengineering 10 (2023) 655, https://doi.org/10.3390/bioengineering10060655.
[105] G. Ashraf, M. Asif, A. Aziz, T. Iftikhar, Z.-T. Zhong, S. Zhang, B. Liu, W. Chen, Y.-D. Zhao, Advancing interfacial properties of carbon cloth via anodic-induced self-assembly of MOFs film integrated with α-MnO_2: a sustainable electrocatalyst sensing acetylcholine, J. Hazard. Mater. 426 (2022) 128133, https://doi.org/10.1016/j.jhazmat.2021.128133.
[106] R.R. Poolakkandy, N.A. Ramalakshmi, K.A. Padmalayam, R.G. Krishnamurthy, M. M. Menamparambath, Braided copper cobaltite/MWCNT composites enable acetylcholine detection at sub-nanomolar levels *in vitro*, Sens. Diagn. 2 (2023) 726–735, https://doi.org/10.1039/D3SD00046J.
[107] F. Amirghasemi, A. Al-Shami, K. Ushijima, M.P.S. Mousavi, Flexible acetylcholine neural probe with a hydrophobic laser-induced graphene electrode and a fluorous-phase sensing membrane, ACS Mater. Lett. 6 (2024) 4158–4167, https://doi.org/10.1021/acsmaterialslett.4c00825.
[108] D. Zhang, J. Ma, X. Meng, Z. Xu, J. Zhang, Y. Fang, Y. Guo, Electrochemical aptamer-based microsensor for real-time monitoring of adenosine in vivo, Anal. Chim. Acta 1076 (2019) 55–63, https://doi.org/10.1016/j.aca.2019.05.035.
[109] H. Chang, M. Huo, Q. Zhang, M. Zhou, Y. Zhang, Y. Si, D. Zhang, Y. Guo, Y. Fang, Flexible needle-type microbiosensor for real-time monitoring traditional acupuncture-mediated adenosine release in vivo, Biosens. Bioelectron. 235 (2023) 115383, https://doi.org/10.1016/j.bios.2023.115383.
[110] J.M. Seibold, S.W. Abeykoon, A.E. Ross, R.J. White, Development of an electrochemical, aptamer-based sensor for dynamic detection of neuropeptide Y, ACS Sens. 8 (2023) 4504–4511, https://doi.org/10.1021/acssensors.3c00855.
[111] N.K. Mintah Churcher, S. Upasham, P. Rice, S. Bhadsavle, S. Prasad, Development of a flexible, sweat-based neuropeptide Y detection platform, RSC Adv. 10 (2020) 23173–23186, https://doi.org/10.1039/D0RA03729J.
[112] J. Aerathupalathu Janardhanan, J.-W. She, H. Yu, Easy-to-engineer flexible nanoelectrode sensor from an inexpensive overhead projector sheet for sweat neuropeptide-Y detection, ACS Appl. Bio Mater. 7 (2024) 8423–8433, https://doi.org/10.1021/acsabm.4c01229.
[113] J. Min, J.R. Sempionatto, H. Teymourian, J. Wang, W. Gao, Wearable electrochemical biosensors in North America, Biosens. Bioelectron. 172 (2021) 112750, https://doi.org/10.1016/j.bios.2020.112750.
[114] T. Saha, R. Del Caño, K. Mahato, E. De La Paz, C. Chen, S. Ding, L. Yin, J. Wang, Wearable electrochemical glucose sensors in diabetes management: a comprehensive review, Chem. Rev. 123 (2023) 7854–7889, https://doi.org/10.1021/acs.chemrev.3c00078.
[115] X. Tong, L. Ga, L. Bi, J. Ai, Wearable electrochemical sensors based on nanomaterials for healthcare applications, Electroanalysis 35 (2023) e202200228, https://doi.org/10.1002/elan.202200228.
[116] B. Zhong, X. Qin, H. Xu, L. Liu, L. Li, Z. Li, L. Cao, Z. Lou, J.A. Jackman, N.-J. Cho, L. Wang, Interindividual- and blood-correlated sweat phenylalanine multimodal analytical biochips for tracking exercise metabolism, Nat. Commun. 15 (2024) 624, https://doi.org/10.1038/s41467-024-44751-z.
[117] H. Teymourian, M. Parrilla, J.R. Sempionatto, N.F. Montiel, A. Barfidokht, R. Van Echelpoel, K. De Wael, J. Wang, Wearable electrochemical sensors for the monitoring and screening of drugs, ACS Sens. 5 (2020) 2679–2700, https://doi.org/10.1021/acssensors.0c01318.
[118] M. Sekar, R. Sriramprabha, P.K. Sekhar, S. Bhansali, N. Ponpandian, M. Pandiaraj, C. Viswanathan, Review—towards wearable sensor platforms for the electrochemical detection of cortisol, J. Electrochem. Soc. 167 (2020) 067508, https://doi.org/10.1149/1945-7111/ab7e24.
[119] R.L. Bulathsinghala, W. Ding, R.D.I.G. Dharmasena, Triboelectric nanogenerators for wearable sensing applications: a system level analysis, Nano Energy 116 (2023) 108792, https://doi.org/10.1016/j.nanoen.2023.108792.
[120] C. Gu, P. Gai, F. Li, Construction of biofuel cells-based self-powered biosensors via design of nanocatalytic system, Nano Energy 93 (2022) 106806, https://doi.org/10.1016/j.nanoen.2021.106806.
[121] G. Nazir, A. Rehman, J. Gautam, M. Ikram, S. Hussain, S. Aftab, K. Heo, S.-Y. Lee, S.-J. Park, Advancements in flexible perovskite solar cells and their integration into self-powered wearable optoelectronic systems, Adv. Powder Mater. 4 (2025) 100304, https://doi.org/10.1016/j.apmate.2025.100304.
[122] M. Parrilla, K. De Wael, Wearable self-powered electrochemical devices for continuous health management, Adv. Funct. Mater. 31 (2021) 2107042, https://doi.org/10.1002/adfm.202107042.
[123] B. Zhang, C. Chen, I. Lee, K. Lee, K.-L. Ong, A survey on security and privacy issues in wearable health monitoring devices, Comput. Secur. 155 (2025) 104453, https://doi.org/10.1016/j.cose.2025.104453.
[124] E.A. Dugan, C. Bennett, I. Tamames, W.D. Dietrich, C.S. King, A. Prasad, S. M. Rajguru, Therapeutic hypothermia reduces cortical inflammation associated with Utah array implants, J. Neural Eng. 17 (2020) 026035, https://doi.org/10.1088/1741-2552/ab85d2.
[125] B.M.G. Rosa, S. Anastasova, G.Z. Yang, NFC-powered implantable device for on-body parameters monitoring with secure data exchange link to a medical blockchain type of network, IEEE Trans. Cybern. 53 (2023) 31–43, https://doi.org/10.1109/TCYB.2021.3088711.
[126] A. Iqbal, P.R. Sura, M. Al-Hasan, I.B. Mabrouk, T.A. Denidni, Wireless power transfer system for deep-implanted biomedical devices, Sci. Rep. 12 (2022) 13689, https://doi.org/10.1038/s41598-022-18000-6.
[127] T. Jiang, Q. Han, H. Wang, X. Jin, L. Xing, Z. Long, X. Xue, L. Li, A wireless-powered implantable sensor for monitoring gastric anastomosis after surgery, Sensors Actuators B Chem. 446 (2026) 138683, https://doi.org/10.1016/j.snb.2025.138683.
[128] H. Kim, B. Rigo, G. Wong, Y.J. Lee, W.-H. Yeo, Advances in wireless, batteryless, implantable electronics for real-time, continuous physiological monitoring, Nano-Micro Lett. 16 (2024) 52, https://doi.org/10.1007/s40820-023-01272-6.
[129] J. Kim, R. Kumar, A.J. Bandodkar, J. Wang, Advanced materials for printed wearable electrochemical devices: a review, Adv. Elect. Materials 3 (2017) 1600260, https://doi.org/10.1002/aelm.201600260.
[130] S. Wang, Y. Liu, A. Zhu, Y. Tian, In vivo electrochemical biosensors: recent advances in molecular design, electrode materials, and electrochemical devices, Anal. Chem. 95 (2023) 388–406, https://doi.org/10.1021/acs.analchem.2c04541.
[131] B. Wolfrum, E. Kätelhön, A. Yakushenko, K.J. Krause, N. Adly, M. Hüske, P. Rinklin, Nanoscale electrochemical sensor arrays: redox cycling amplification in dual-electrode systems, Acc. Chem. Res. 49 (2016) 2031–2040, https://doi.org/10.1021/acs.accounts.6b00333.
[132] Y. Wang, Z. Liu, J. Li, C. Ge, X. Ye, Y. Xie, P. Zhao, J. Fei, Polyaniline-on-MOF protects the MOF structure during carbonization for the construction of a portable sensor to detect tert-butylhydroquinone, Nano Energy 135 (2025) 110655, https://doi.org/10.1016/j.nanoen.2025.110655.
[133] Y. Dai, X. Kan, From non-electroactive to electroactive species: highly selective and sensitive detection based on a dual-template molecularly imprinted polymer electrochemical sensor, Chem. Commun. 53 (2017) 11755–11758, https://doi.org/10.1039/C7CC06329F.